Title
Engineering a Highly Adhesive and Hemostatic Sealant for Soft Tissues

Author
Baghdasarian, Sevana

Publication Date
2020

Peer reviewed|Thesis/dissertation

UNIVERSITY OF CALIFORNIA

Los Angeles

Engineering a Highly Adhesive and Hemostatic Sealant for Soft Tissues

A thesis submitted in partial satisfaction

of the requirements for the degree of Master of Science

in Chemical Engineering

by

Sevana Baghdasarian

2020

ABSTRACT OF THE THESIS

Engineering a Highly Adhesive and

Hemostatic Sealant for Soft Tissues

by

Sevana Baghdasarian

Master of Science in Chemical Engineering

University of California, Los Angeles, 2020

Professor Nasim Annabi

The existing surgical adhesives and sealants lack strong adherence to the biological tissues in the wet environment. In addition, demonstrating both inherently high adhesion and hemostatic functionalities in one product, is a scarce characteristic of the developed biomaterials. Moreover, to eliminate the physical and mechanical mismatches with native tissues, high tuning ability is desirable but limited in the current products. As a result, the current solutions fail to either close the wound, or maintain a sufficient sealing ability during wound healing. In this work, a novel and efficient synthetic technique was successfully developed to chemically conjugate catechol motifs to the gelatin backbone. The resulting gelatin-catechol compound was then chemically functionalized with methacryloyl groups to form a highly adhesive and photocrosslinkable sealant, named gelatin methacryloyl-catechol (GelMAC). A two-step crosslinking approach was employed

to form the double-networked, and highly tunable GelMAC hydrogel system. First, different concentrations of Fe^{3+} ions (0, 1, 2.5, 5 and 10 μM) were introduced to the 20 %(w/v) GelMAC prepolymer solution. This step was followed by a second crosslinking mechanism utilizing visible light photopolymerization. GelMAC hydrogel with 2.5 μM Fe^{3+} ion concentration (GelMAC-Fe) was found to have lower elastic and compressive moduli but demonstrated comparable extensibility to Gelatin-methacryloyl (GelMA) hydrogel incorporating the same Fe^{3+} ion concentration (GelMA-Fe). Moreover, the wound closure test with porcine skin showed a 1.5-fold higher adhesive strength for GelMAC-Fe compared to GelMA-Fe hydrogels. To study the hemostatic efficacy of GelMAC-Fe hydrogel, the time lapse of blood coagulation across experimental groups was studied *in vitro*. While the negative control group (untreated blood) formed a blood clot after 16 min, GelMAC hydrogels decreased the clotting time significantly to 9 min. These results were also in close agreement with those obtained for the commercially available hemostatic material, SURGICEL®. Finally, the results of the *in vivo* liver bleeding model showed that GelMAC-Fe hydrogel was able to rapidly crosslink the incision site and stop the bleeding faster compared to other hydrogels. GelMAC-Fe hydrogel exhibited superior adhesion strength while offering significant hemostatic ability owing to the presence of ferric ions (Fe^{3+}) and the dopamine molecule. This novel, highly biocompatible, tunable, adhesive, and hemostatic sealant can therefore be utilized as an effective solution for controlling bleeding and sealing of soft internal organs such as the lung, heart and blood vessels.

The thesis of Sevana Baghdasarian is approved.

Harold G. Monbouquette

Junyoung O. Park

Nasim Annabi, Committee Chair

University of California, Los Angeles

2020

To My Family

TABLE OF CONTENTS

LIST OF FIGURES

LIST OF TABLES

ACKNOWLEDGEMENTS

This project was supported by the National Institutes of Health (R01-EB023052; R01HL140618).

Sections 1, 3, and 4 are a version of sections of publication in preparation.

Section 2.3 is a version of a section of publication in preparation.

I would like to immensely thank the following individuals for their contributions in this project: Bahram Saleh (contributed in drafting sections 1, 3, 4, assisted in NMR data analysis, contributed to drawing of figure 4.1A), Avijit Baidya (NMR data and analysis, contributed in writing sections 1, 3, 4, optimization studies, contributed to drawing of figures 4.1A, and 4.3A), Hanjun Kim (*in vivo* hemostatic efficacy studies and data analysis), Mahsa Ghovati (burst pressure test, assisted *in vitro* swelling and degradation studies, and data analysis), Ehsan Shirzaei Sani (data analysis), Reihaneh Haghniaz (*in vitro* hemostatic assay and data analysis), and Dr. Nasim Annabi (project PI).

1. Introduction

Recently, the Centers for Disease Control and Prevention (CDC) have estimated that approximately 30 million surgical procedures are being performed annually in the United States, alone [1]. Most of these procedures involve incisions from 1-2 cm in size in the case of minimally invasive surgery, to 10–20 cm or greater in other cases. Larger surgical wounds can potentially facilitate chronicity and complications such as surgical site infection (SSI), prolonged hospitalization, increased cost, morbidity and mortality, and decreased quality of life. In addition, surgical wounds possess greater risk for the patients who are experiencing host defense misfunctioning issues such as diabetes, autoimmune diseases, cancer, and others.

Traditionally, surgical wound closure procedures include the use of sutures, staples, or wires. However, using these techniques, particularly for parenchymatous tissues such as lungs, liver, or kidney, is still a challenge. In addition, suturing such fragile tissues often leads to necrosis and dehiscence of the wound. Apart from this, surgical procedures are always coupled with other common complications related to hemorrhage, triggering severe health complications due to the uncontrolled blood loss. Even minimally invasive procedures may lead to significant complications arising from a small amount of bleeding (e.g. compromising the vision during ocular procedure) [2]. Thus, hemostatic sealants have become key components of the surgical toolbox to manage residual bleedings despite the application of conventional methods for hemorrhage control [3, 4]. Therefore, developing a biomaterial having both hemostatic and wound sealing ability, will be tremendously beneficial.

Today, in the era of sutureless surgical procedures, fibrine-, collagen- and cyanoacrylate-based adhesives are well-known and intensely utilized for various clinical wound closure applications. Despite all the advantages that the naturally derived fibrin and collagen-based adhesives have to

offer, these materials lack efficient adhesion and cohesion properties. Moreover, the use of fibrin glue may introduce the risk of possible blood-borne disease transmission and cause potential allergic reactions in the patients. In contrast, despite their high adhesive and mechanical properties, cyanoacrylate-based synthetic glues have exhibited considerable concerns related to their exothermic polymerization reaction, slow degradation rate, toxicity, and increased tissue inflammations. Meanwhile, hydrogel-based materials having tissue-like physical properties, hold remarkable potential to be used as surgical sealants and bioadhesives [5]. However, in most cases the developed hydrogels exhibit weak tissue adhesion in clinically relevant physiological environments such as wet tissue surfaces. Although a few polymer-based adhesives have been developed that function well in the wet environments [6, 7], their clinical application is limited due to several parameters. These include long gelation time, long and multi-step synthesis process [7], uncontrolled polymerization and difficulties in material handling during application, inability to control extensive bleeding, non-elasticity, low adhesion, and issues related to their biocompatibility and biodegradability. Therefore, there is an existing need to enhance the current limitations of hydrogel-based materials for wet tissue adhesion and sealing applications.

To enhance the wet-adhesion ability of the biopolymer-based hydrogels, the mussel-inspired adhesion mechanism was utilized by incorporating catechol moieties [8-10]. The feasibility of these catechol moieties to enhance adhesion in wet environments has previously been demonstrated [11-13]. The catechol moieties facilitate the formation of chemical and physical bonding with the tissue surfaces [14]. Considering these unique properties, various kinds of catechol-incorporated bioadhesives have been successfully designed for different biomedical applications including wound sealing and repair, antimicrobial coating, cancer treatment, etc. [15, 16]. For example, recently, a catechol modified gelatin-based injectable hydrogel was introduced

having considerable biocompatibility and tissue adhesive property [17]. However, this material lacked significant mechanical strength associated to the crosslinking mechanism of the developed hydrogel. Therefore, not only it is essential to develop successful chemistries to incorporate catechol moieties and arrive at a highly adhesive biopolymer, but it is also crucial to achieve this outcome without comprising the mechanical strength of the resulting hydrogels.

Controlling bleeding which typically concurs with tissue injury, is a critical step during wound closure. Mechanistically, while active hemostatic agents, such as fibrinogen and thrombin, facilitate particular pathway of coagulation cascade, mechanical hemostats (e.g. collagen-, cellulose- based hemostats) enable various functional interactions with the tissue and accelerate the clot formation [2, 18]. Although, most of the commercially available hemostatic agents (e.g., SURGICEL®) control the bleeding and stimulate clotting, they do not possess adhesive properties and fail to reconnect the injured tissues or the wound site. Thus, designing a biocompatible, biodegradable, and mechanically stable hydrogel exhibiting significant adhesion to the wet biological surfaces while promoting hemostasis, and facilitating tissue healing is desired for the management of internal wounds.

Recently, these adhesive hydrogel materials are also functionalized with various inorganic and organic molecules that actively provide hemostasis and control the bleeding from the raptured tissue surfaces. These include incorporation of hemostasis agents in the hydrogel to enhance the therapeutic efficiency [19]. For instance, keratin-based QuikClot [20] and gelatin and thrombin based Floseal [21] that promote clotting in an injectable form and commercially available. Among the inorganic nanoparticles, zeolite and silicates are well-known in this context. For instance, laponite nanoplates having enormous surface charges, assist the strong electrostatic interaction mediated rapid blood coagulation. Various nature derived biopolymers such as chitosan, having

polycationic structural backbone, enables nonspecific binding to cell membranes [18] and easily forms a coagulum in contact with the whole blood. However, uncontrolled interaction of chitosan with inflammatory cells has led to a strong foreign body response and complete degradation of these hydrogels within three days [22, 23].

To address the above limitations, a hemostatic adhesive material, named gelatin methacryloyl-catechol (GelMAC) has been developed through the incorporation of biologically-inspired catechol motifs and photocrosslinkable MA functionalities on the gelatin backbone in a one-step reaction. GelMAC hemostatic sealant was formed by first adding the Fe^{3+} ions to crosslink the catechol groups followed by photocrosslinking of the methacrylated groups to form a double network hydrogel system. This improved the mechanical and adhesion properties of the material. In addition, it is shown that the physical properties and adhesion strength of the resulting GelMAC bioadhesives could be tuned by changing the Fe^{3+} ion concentration. Moreover, the presence of Fe^{3+} ions could provide hemostatic characteristics to the engineered hydrogel system. The physical properties of the engineered hemostatic sealants including mechanical, swelling and degradability, adhesion, and rheological profiles were fully characterized. In addition, the *in vitro* biocompatibility of GelMAC hydrogels was studied utilizing NIH 3T3 fibroblast cells. Moreover, the biocompatibility and *in vivo* capability of the developed hydrogels to control the bleeding was studied in a rat subcutaneous model, and a liver bleeding model, respectively. The GelMAC bioadhesive showed excellent potential to be used as a highly adhesive hemostatic sealant. In this work, 3,4-dihydroxyphenylalanine (dopamine) and methacrylate groups were covalently linked with carboxylic acid and amine functionalities on the gelatin backbone, respectively. In addition, incorporated catechol groups contribute to secondary crosslinking through the chelation with Fe^{+3} ions [24, 25], and improve the mechanical strength of the material. Therefore, it is hypothesized

that the addition of Fe^{3+} ions will result into rapid blood coagulation in both *in vivo* and *ex vivo* experiments and will deem the engineered adhesive hydrogel hemostatic also.

2. Background

2.1 Wound Healing

Wound healing is a biological process occurring in response to tissue injury. The wound healing is natural occurring protective mechanism from harmful external environmental toxins and pathogens. Wound healing is known to occur in four integrated and highly programmed stages. These stages are hemostasis, inflammation, proliferation and remodeling (Figure 2.1)

During the Hemostasis stage clotting of the blood occurs to close the wound. Hemostasis starts when the blood rushes out of the body to the location of the wound (Figure 2.1A). The first respond of the body after the blood leakage occurs is when blood vessels constrict to restrict future blood flow. The next step after the blood vessels contractions is the adhesion of platelets at the location of the wound together to seal the break in the wall of the blood vessel. After the palettes adhere to the sub-endothelium surface, the first fibrin which are like a molecular binding agent strands begin to adhere and form a fibrin network. As the fibrin stands adhere to the epithelial wall and form a fibrin network, the blood transforms from its liquid phase to gel phase through pro-coagulants and thrombus or clot is formed. The newly formed clot keeps the platelets and blood cells trapped in the wound area which is essential in the pro-inflammation and wound healing.

Inflammation stage of the wound healing proceeds hemostasis stage to control the bleeding and prevents infection after the injury (Figure 2.1B). After the injury, the blood vessels fluid leak out resulting localized swelling. In this stage, the damaged cells and pathogens or bacteria are removed

from the wound area while the healing and repair cells and blood cells (neutrophils, monocytes, and macrophages), growth factors, proinflammatory cytokines, chemokines, nutrients and enzymes move to the site of the wound. The presence of white blood cells, growth factors, nutrients, enzymes, and histamines (other amines) create the swelling, heat, pain and redness at the site of the wound.

In the proliferative stage, a new matrix of collagen fibers, proteoglycans and fibronectin are replaced with the fibrin matrix to restore the structure and function of the injured tissue (Figure 2.1C). In addition, angiogenesis (in-growth of new capillaries) in order to supply granulation tissue sufficient oxygen and nutrients. In the proliferative stage, fibroblast play an important role. Fibroblasts migrate to the site of injury in response to platelets and macrophages. The fibroblasts migration to the wound site requires them to change their shape and also secrete proteases to clear their way into the wound site. in order to make it to the presence of myofibroblasts cause the wound to contract by gripping the wound edges and pulling them together in order to minimize surface area and bring the cells at close proximity. It is known that the granulation tissue color is pink and is resistant to bleeding. Any discoloration is not normal and is a sign that the wound is being infected, ischemic or had a poor perfusion. At the end of the proliferation stage the epithelial cells resurface to the site of the injury and rebuilt their structure. For a successful epithelialization the environment is well known to keep at moisture and hydrated.

Remodeling is the final stage of wound healing (Figure 2.1D). In remodeling stage, the collagen is remodeled from type III to type I and therefore the wound fully closes. The cells that were present at the location of the wound for repair that are no longer needed undergo apoptosis to clear the location of the wound. In the remolding stage, the collagen structure also becomes mature and become close together and cross-link. The remodeling stage of wound healing can also take a long

time. Over several months, changes or remolding of the healed wound will slowly increase the tensile strength to a maximum of about 80% of the normal tissue.

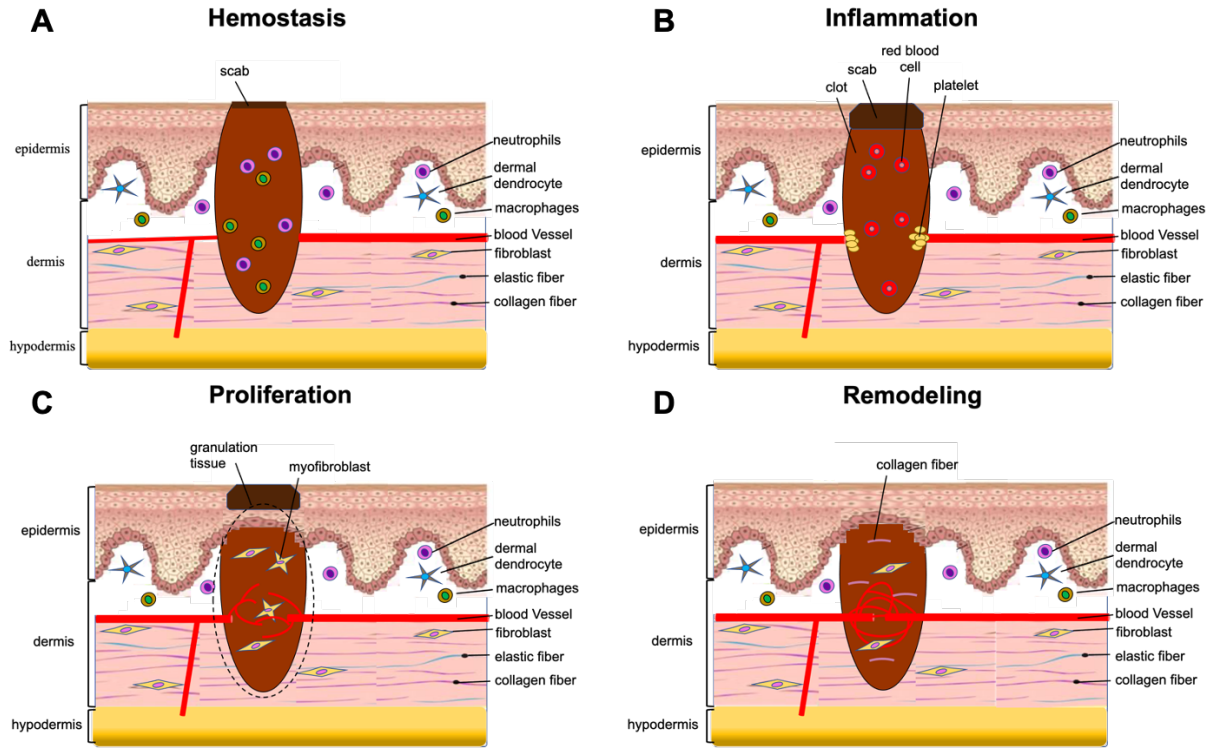

Figure 2.1 The 4 stages of the wound healing. A) Hemostasis. B) Inflammation. C) Proliferation. D) Remodeling.

2.2 Adhesive Sealants

Biopolymer based hydrogels have been extensively researched in recent decades due to their potential utility in clinical applications [26-29]. These materials are frequently used in 3D printing, wound healing, transplantation, drug delivery and for various other applications [30-37]. The use of biopolymers has also been demonstrated in the area of bio-adhesive research and have proven their potential applicability and feasibility in forming adhesive hydrogels [8, 38-40]. Not only naturally derived biopolymers contain enormous number of chemically functionalizable groups, but these biopolymers can also be decorated with various other molecules to enhance the facile

interactions between the hydrogel and hydrophilic tissues surfaces [41, 42]. Such chemical interactions include both non-covalent interactions such as various hydrogen bonding and electrostatic interactions, π-π interaction, as well as covalent interactions namely in-situ formation of C-C bond, S-S bond, depending on the biopolymer [14]. In most cases, these interactions are facilitated with various light induced chemical crosslinking processes and/or ion induced chelation mechanism. While functional groups such as hydroxyl (-OH), amine (-NH2), carboxyl (-COOH), and thiol (-SH) are responsible for non-covalent interactions, chemically attached C=C groups take part in photo-crosslinking, forming C-C bonds. In addition, aromatic groups such as benzene moieties and aliphatic chains are responsible for π-π interaction and weak Van der Waal interactions [14]. These impart both adhesive property and structural integrity of the material at the same time. Meanwhile, in order to best suit as a desirable bioadhesive candidate, biopolymer based hydrogels are often designed and optimize to closely mimic the chemical and physical characteristics of the native tissues. For example, a hydrogel material designed for lung tissue regeneration needs to possess characteristics such as softness and elasticity. Whereas for the nerve tissue application, high conductivity and elasticity are desirable at the same time. Therefore, it is very important to tune the physical properties of the developed material to avoid any mechanical mismatch which could lead to complications or failure.

Typically, the physical properties of a hydrogel material are solely determined with the functional groups present on the polymer backbone and their interactions within the hydrogel system. For example, polymers having hydrophobic groups impart elasticity to the hydrogel material though the deformable and reversible non-covalent interactions [14]. In this regard, elastin like peptide molecules with hydrophobic functionalities have been utilized to develop photocrosslinkable adhesive hydrogels with enhanced extensibility and mechanical properties [43]. Similarly, other

naturally derived elastomeric hydrogels such as chemically crosslinked tropoelastin hydrogels, photocrosslinkable tropoelastin hydrogels, and animal-derived elastin hydrogels have been developed for biomedical applications [44]. Notably, the methacryloyl-substituted tropoelastin (MeTro) has shown excellent biocompatibility and high extensibility up to 400% [45]. As another example, biopolymers such as alginate provide fast and strong/rigid hydrogel formation. Particularly, in this case, the presence of -COOH (carboxylic) groups readily interact with metal ions through the chelation process [7]. These biopolymers are either chemically linked or physically mixed with other molecules or materials to evolute the desire properties of the hydrogel. For example, dopamine molecules were chemically conjugated with different biopolymers to develop a naturally inspired adhesive hydrogel [38]. In addition, recently, Moshaverinia et al. have been able to chemically conjugate dopamine and RGD functional groups to the oxidized alginate to develop an adhesive hydrogel that promotes craniofacial bone tissue regeneration [46]. The developed hydrogels have shown excellent biodegradability, biocompatibility, and osteoconductivity, and have been utilized for the delivery of mesenchymal stem cell (MSC). In order to improve the mechanical strength of the hydrogels, multiple polymeric materials have been incorporated, physically mixed, and in-situ polymerized. For example, methacrylated gelatin and methacrylated alginate based functional polymers ware mixed to enhance the intermolecular interactions through the formation of visible light activated C-C bonds formation [7]. Similarly, inorganic laponite nano silicates have also utilized by mixing with prepolymer solutions to improve the mechanical properties of the resulting adhesive hydrogels [47-49]. Moreover, to develop a conductive adhesive hydrogel, prepolymer solutions have also been physically mixed with graphene oxide, bio-ionic liquids, and other conducting materials. For example, Khademhosseini et al. have developed a GelMA-based conductive hydrogel with graphene oxide

[50]. In this case, GelMA molecules were able to readily interact with the graphene oxide and act as a biocompatible surfactant. This hydrogel system was demonstrated to exhibit tunable physical properties and enhanced cellular behavior, both of which are highly important criteria of design considerations for tissue engineering applications. Finally, Bio-Ionic Liquid (Bio-IL) incorporated hydrogels have been designed and developed by Noshadi et al. where ionic liquid interacts with the polymeric backbone resulted into the formation of covalent linkages [51].

Apart from the naturally derived biopolymers, various synthetic polymers have been developed and utilized as adhesive sealants. In most cases, these synthetic polymers were incorporated in the formulation in order to improve certain physical properties of the hydrogel system such as stretchability, adhesive property, conductivity, etc. For example, poly(glycerol sebacate acrylate) based hydrophobic polymers have been used to develop elastic and biocompatible adhesive materials [52]. Due to their hydrophobic nature, these hydrogels exhibited less swelling and better adhesion in wet environment. In addition, the developed UV-crosslinked hydrogels showed strong adhesion in dynamic environments and under prolonged bleeding condition. Recently, a bi-layered tough adhesive material was designed by Mooney et al. which was shown to have excellent adhesion within a minute of application and was found to be a suitable candidate in diverse biomedical application including wound dressing, and tissue repairing [53]. In this study, while one layer adhered to the tissue surface by electrostatic interactions, covalent bonds, and physical interpenetration, the second layer provided easy energy dissipation. Swelling of the adhesive material in physiological condition being a major drawback due to the mechanical weakening, catechol-modified amphiphilic poly(propylene oxide)-poly(ethylene oxide) block copolymers was used to synthesize a mechanically robust, negative-swelling hydrogel material. Finally, stretchable

and tough adhesive (polyurethane-based) hydrogel have been designed [54, 55]. However, the biocompatibility and biodegradation of these materials are still a design limitation.

2.3 Hemostatic Sealants

2.3.1 Commercialized Hemostatic Sealants

Over the last few decades, several commercial products have been developed to meet the arising demands for hemostatic sealants in various clinical applications. These FDA-approved products are developed and approved for specific indications as noted in Table 2.1. Although some of these products offer great advantages compared to the traditional treatments, limited elasticity, inadequate stiffness, and low tissue adhesion, particularly in wet and highly dynamic physiological environments in the presence of blood, are some of the limitations associated with them. For example, cyanoacrylate-based sealants possess high adhesive strength, but exhibit much higher stiffness compared to native tissues in addition to the cytotoxicity issues related to their utility for internal use [56, 57]. A few of the commercially available hemostatic agents (e.g., TISSEEL and EVICEL®) rely on the use of gelatin or fibrin as a sealing matrix while incorporating thrombin and coagulating factors (factor XIII) to achieve hemostasis. Although highly biocompatible, however, these hemostatic agents do not possess adequate mechanical and adhesive properties [58]. In addition, adhesives with thrombin as a hemostatic agent rely on the patient's innate coagulatory response which in certain cases could be compromised. Moreover, hemostatic sealants containing thrombin and fibrinogen may pose the risk of introducing strong coagulation activators into the blood stream [59]. Commercially available products, therefore, often fail to provide appropriate sealing capabilities and hemostatic properties simultaneously. As such, other hemostatic sealants are under development to fulfill the current gaps.

Table 2.1 Commercialized hemostatic sealants

Product Name	Materials	Indicated Application	Curing Time	Application Method	Disadvantages
TISSEEL (P103980)	▪ Human fibrinogen ▪ Thrombin ▪ Bovine fibrinolysis inhibitor	▪ Cardiopulmonary bypass	▪ 2 minutes	▪ Spray	▪ Risk of disease transmission ▪ Associated with skin rash, allergy, or anaphylaxis
EVICEL® (BL 125010)	▪ Human fibrinogen ▪ Thrombin	▪ Liver/HPB procedures ▪ Orthopedic surgeries	▪ 10 minutes (to achieve hemostasis)	▪ Spray ▪ Drip	▪ Risk of disease transmission ▪ Low burst pressure, adhesion, and elasticity
BioGlue® (P010003)	▪ Bovine serum albumin ▪ Glutaraldehyde	▪ For open surgical repairs of aorta, femoral, and carotid arteries	▪ 2 minutes	▪ Extrude	▪ High toxicity of glutaraldehyde ▪ Not elastic
ArterX®, PREVELEAK™ (P100030)	▪ Bovine serum albumin ▪ Polyaldehyde	▪ Vascular reconstruction	▪ 10 minutes	▪ Extrude	▪ High toxicity of glutaraldehyde ▪ Delayed healing ▪ Release of toxic by-products
CoSeal™ (P030039)	▪ Glutaryl-succinimidyl ester ▪ Thiol terminated PEG	▪ Vascular reconstruction	▪ 10 minutes (forms a gel in <3 seconds)	▪ Extrude	▪ Low adhesion, burst pressure, shear strength, and elasticity ▪ Risk of Swelling
Ethicon™ OMNEX™ (P060029)	▪ 2-octyl cyanoacrylate ▪ Butyl lactoyl cyanoacrylate	▪ Vascular reconstruction	▪ 2 minutes	▪ Extrude	▪ Mild immunohistopathological reactions ▪ Toxic by-products

2.3.2 Under Development Hemostatic Sealants

2.3.2.1 Applications in Wound Healing

It is an important and highly desired to control bleeding from the wound site caused by traumatic injuries, or during surgical procedures. Although various materials are well-known in the clinical realm, most of them possess inherent limitations such as low biocompatibility, lack of hemostasis related to cytotoxic and immunogenic components, and many others. One of the prominent issues of hemostatic agents is related to the instability of the material during the blood flow. Typically, these materials lack cohesion integrity and possess adverse adhesion capability over the injury site. In order to address such limitations, hemostatic materials with adhesive ability have been pursued and developed. For instance, in a recent study by An et al. a bio-inspired, novel and highly biocompatible hemostatic adhesive have been engineered which relies on platelet clotting mechanism [60]. The serotonin-conjugated hyaluronic acid (HA-serotonin) hydrogel exhibited improved hemostatic ability *in vivo* in a mouse liver hemorrhage model (both normal and hemophilic injuries) when compared to a commercially available fibrin-based hemostatic agent. Detailed histological analysis has also showed the formation of blood clot even in the wound area of hemophilic mice. This reflects the potential utility of the material in clinical applications especially due to the fact that it is driven by the synergistic effect of platelet activation and the physical barrier. Most importantly, the developed biomaterial prevented the abnormal tissue-adhesion through the anti-biofouling effects of cohesive hyaluronic acid hydrogel. Moreover, the utility of this bio-inspired multifunctional hemostatic adhesive is deemed expandable to tissue engineering scaffolds and drug delivery carriers. Meanwhile, another multifunctional bioadhesive has been

engineered by Zhu et al. which is based on polysaccharides and peptide dendrimers, offering rapid crosslinking and high strength capabilities [61]. In addition to offering high biocompatibility, and good antimicrobial properties, the novel aldehyde/amine-mediated bioadhesive was shown to have effectively reduced the blood loss when compared to Coseal^{TM} in a rat liver hemorrhage model. Such hemostatic properties of the hydrogels have been attributed to both their flexible mechanical sealing performance as well as the hemostatic mechanism of OCMC. In this study, the OCMC/G3KP hydrogels were deemed to exhibit superior and accelerated wound healing efficacy when tested *in vivo* utilizing a full thickness rat dorsum incision model. In this case, although the histology data with hematoxylin and eosin (H&E) staining showed initial acute inflammation both for the material and control, the engineered material promoted complete wound healing in addition to the formation of blood vessels and dermis, negligible cell infiltration, and lack of any visible fibrosis. Therefore, the ability to form rapid covalent bonding interaction with tissue surface at the incision site makes this adhesive biomaterial an excellent candidate for clinical wound closure applications. Furthermore, to achieve rapid hemostasis, Shou et al. have pursued the design and development of biocompatible and strongly tissue-adhesive hydrogels with short in situ gelation time at body temperature to serve as anti-hemorrhaging barriers to bleeding wound tissues [62]. The hemostatic efficacy of the engineered hydrogels was studied in an *in vivo* rat liver bleeding model with the results supporting a significant reduction in bleeding time and bleeding mass compared to those of untreated group. The resulting adhesive hydrogel system could strongly adhere to the tissue through several interactions, requiring only a 30s gelation time when temperature was elevated to 37^{o}C. Recently, an injectable multifunctional

composite hydrogel engineered by Liang et al. has exhibited excellent hemostasis along with superior adhesive, antioxidant, and conductive properties [63]. Interestingly, rGO and HA-DA-based nanocomposite possesses native human skin tissue-like property and was used for full-thickness skin regeneration during wound healing. This adhesive conductive hydrogel was found to have good adhesive strength *in vivo*, comparable, or even better than commercial Tegaderm film dressings. To demonstrate the applicability of the hybrid hydrogel on real tissue surfaces and homeostatic conditions, HA-DA/rGO hydrogels was tested in a liver bleeding mouse model and showed good hemostatic capacity. In addition, the excellent photothermal antibacterial property as well as bioactivity of polydopamine facilitates the feasibility of the material as a bioactive wound dressing candidate.

2.3.2.2 Applications in Heart and Arteries

In clinical field, a strong and rapid underwater adhesion is desired for different wound closure applications in wet conditions. This feature is highly sought after especially in open procedures such as those involving heart and arteries. In this regard, an injectable hemostatic sealant with such ability is in high demand. Recently, Cui et al. has developed a highly adhesive hemostatic sealant based on pentaerythritol tetra-acrylate (PETEA), poly(ethylene glycol) diacrylate (PEGDA-200) and dopamine [64]. The resulting hydrogels can rapidly stop visceral bleeding while strongly adhering to the wound site. Novel sealant material is consisted of a hydrophobic backbone and hydrophilic adhesive catechol side branches which triggers the rapid adhesion upon contact with water. Two distinct models, femoral artery bleeding and liver bleeding in rats, were utilized to study the hemostatic effect of the bioinspired hydrogels concluding that the bleeding was quickly

and completely stopped with almost no detectable bloodstain. Subcutaneously implantation in the rat's body showed complete degradation of the material without any indication thrombosis. Meanwhile, the material was described to be more useful towards the irregular and deep wounds due to its easy injectability which restrict the application of solid hemostatic materials. Similarly, Hong et al. has designed another highly biocompatible adhesive hemostatic hydrogel specifically for the repair of the injured arterial and heart bleeds [65]. Gelatin-metacrylol (GelMA) and glycosaminoglycan hyaluronic acid (HA-NB) based this material rapidly seal the bleeding site upon photocrosslinking with UV irradiation. A series of *in vivo* experiments were performed to study the efficacy of developed hydrogels in both rabbit (liver and artery) and pig (carotid arteries and heart). The hemostatic and wound-sealing performance of the GelMA/HA-NB matrix gel was determined to be significantly higher than commercial Fibrin Glue and Surgiflo^{TM}. Moreover, the results obtained from burst pressure tests indicated that the repaired sites could withstand blood pressures up to 290 mm Hg which is significantly higher than systolic blood pressures in most clinical settings. The GelMA/HA-NB adhesive exhibited good biocompatibility and diminished cytotoxicity when subcutaneously implanted in a rat model. Altogether, the GelMA/HA-NB matrix hydrogel is deemed a radically improved hemostatic sealant. Tolerance to blood exposure being a key parameter towards the hemostasis, recently, a silk-based and bioinspired hemostatic sealant was designed and developed by Bai et al. [66]. The *in vivo* hemostatic capacity of the SFT hydrogels were tested in a rat liver bleeding model as well as in a rat heart bleeding model. The results demonstrated that the SFT hydrogels instant hemostatic capacity (within 30 s) and tough adhesion in wet and dynamic conditions. Interestingly, the

developed material showed advanced adhesion on the injury sites having blood rather than water. Owing to their instant co-assembly ability and tough adhesion to mechanically robust bleeding tissues, the SFT hydrogels can serve as a feasible candidate for their potential in wound closure and surgical sealing applications.

2.3.2.3 Other Applications

Recently, *in vivo* tail cut models have extensively been used to demonstrate the hemostatic activity of the material (8). For instance, Krishnadoss et. al has incorporated an ionic liquid moiety in the hydrogel system that improves the hemostasis and tissue adhesive strength of the material together. Performance of the hybrid material was measured in class I hemorrhage (the tail cut) and class II hemorrhage (the liver wedge resection) in a rat model. While on the former case rapid blood clotting was observed in 2 min, it took almost 7 min to promote complete hemostasis in the later experiment. Excellence of the material was further showcased with the Class IV hemorrhage treatment which is known to cause severe hemodynamic instability in human system. Therefore, limits the obvious operative intervention towards various critical bleeding situations. *In vivo* degradation and morphological changes being important parameter, were characterized upon subcutaneous implantation into rats. Detailed study implied no significant macrophage infiltration followed by adverse inflammatory responses. Similar ionic gel-like complex was engineered with of poly((trimethyl- amino)ethyl methacrylate chloride-co-sulfobetaine methacrylate) (poly(TMAEMA-co-SBMA)) and kosmotropic polyphosphate (PP) which showed an important antimicrobial property along with the removable tissue adhesion [67]. During the biological experiments, the material having ionic backbone readily binds

to the various cells through the profound electrostatic interaction. Finally, the hemostatic activity of the material was demonstrated using tail-bleeding assay on Wistar rats and reflects the potential applicability of the same in biomedical field.

Recently, supramolecular coacervate hydrogel (TAHE) based hemostatic material was developed by Zhang and coworkers that exhibits strong adhesion, at the same time [68]. Hemostasis was performed using rat-tail amputation model and rat liver bleeding model where synthesized material adsorbed the blood plasma from the incision and trigger the aggregation induced blood coagulation process. Notably, during the surgical procedure developed material forms a strong physical barrier by transforming itself to a sticky adherent which covered the damaged tissue and facilitates the blood coagulation. Additional self-healing and antibacterial properties of the material have made this to be a potential candidate for several medical emergencies as well. Chemically, extended intra and inter molecular hydrogen bonding interactions plays an important role. Current development of a conductive hydrogel with *in vitro*/*in vivo* photothermal activity was also displayed considerable hemostatic efficacy [69]. This is described in the mouse tail amputation model, mouse liver incision model, and mouse liver trauma model. During the *in vivo* study, intrinsic pathway towards the successful blood coagulation was observed to be greatly influenced with negative charge of the functional group present in the hydrogel matrix. It reinforced *in situ* platelet plug through the formation of stable fibrin which act immediately in the initial hemostasis phase. However, adequate adhesiveness of the hydrogel along with the incorporation of CNT contributed significantly to build active barrier inhibiting the blood flow from the wound sites.

Similar to the liver, heart, tail model in rat, various other models have also been used to demonstrate the hemostatic activity of the developed material. For instance, recently, Gao and coworkers have engineered a chemically modified chitosan based adhesive hydrogel material that provides considerable hemostatic activity during the tests over the artificially created wound sites on rates belly [70]. Catechol and lysine grafted biomacromolecules showed considerable wet tissue adhesion and biocompatibility. Meanwhile, polydopamine (PDA) based hybrid hydrogel material was developed for the application in skin tissue engineering [71]. Here, alkaline polymerization of dopamine molecules followed by the complexation with sodium alginate and polyacrylamide has introduced elasticity and improved mechanical properties. As-synthesized material has exhibited rapid blood coagulation, promoting the hemostasis ability of the mussel-inspired hydrogels. Apart from this material also showed excellent the cell proliferation, cell attachment, cell spreading, and functional expression of human skin fibroblasts (CCD-986sk) and keratinocytes. Table 2.2 summarizes the current under development studies on hemostatic sealants.

Table 2.2 Hemostatic sealants under development

Material	Significant Characteristics of the Developed Hemostatic Sealant	Study Subject and Model	Application	Study Outcomes	Ref
PEGDA MAETMAC Silica particles	▪ Exhibited hemostatic, and antibacterial properties with excellent cytocompatibility and very high water absorption capacity (~5000%) ▪ Was able to promote blood cell aggregation ▪ Facilitated plasma coagulation	▪ Rat-tail	▪ Local hemostatic agent for potential utility in emergency bleeding ▪ Wound healing	▪ Promoted blood cell aggregation and facilitated plasma protein activation via haemadsorption ▪ CSH-MS1 (with approximately 5.06% contents of MS) significantly reduced the bleeding time and the amount of blood loss in a rat-tail amputation model	[72]
BIL (choline bitartrate and acrylic acid) Conjugated GelMA or PEGDA	▪ High adhesion capacity ▪ Potential application in mechano-transduction	▪ Rat tail-cut ▪ Rat liver wedge	▪ Traumatic injury tissue repair ▪ Wound dressing ▪ Attachment of flexible electronics	▪ Exhibited a close to 50% decrease in the total blood volume loss in tail cut and liver laceration rat animal models compared to the control	[73]
Poly((trimethyl-amino)ethyl methacrylate chloride-co-sulfobetaine methacrylate) (Poly(TMAEMA-co-SBMA)) Kosmotropic polyphosphate	▪ Formed stable dispersive colloids and gel-like complexes ▪ A robust, substrate-independent, water based, repeatable, and removable adhesive	▪ Rat-tail	▪ Wide spectrum of applications as surgical sealant	▪ The complex gels served as an antimicrobial agent (inactivated pathogenic bacteria via leaching and contact killing) ▪ The gel-like complex was applied onto various substrates as an adhesive and was compared to commercial superglue gel, exhibiting robust and superior adhesive properties	[67]

Material	Significant Characteristics of the Developed Hemostatic Sealant	Study Subject and Model	Application	Study Outcomes	Ref
Poly(N-hydroxyethyl acrylamide) (PHEAA) Tannic acid (TA)	▪ Strong hydrogen-bonding induced coacervate adhesion to various substrates ▪ Possessed good self-healing ability, plasticity, antibacterial and hemostatic activities ▪ Could be produced and used in the form of powder while retaining its adhesive and hemostatic properties	▪ Rat liver ▪ Rat-tail amputation	▪ Hemostatic adhesive for emergency use	▪ Exhibited self-healing and antibacterial properties ▪ Was shown to have strong adhesion to various substrates, with average adhesion strengths of 722 kPa, 522 kPa, 484 kPa, and 322 kPa to the substrates of iron, PMMA, ceramics, and glass, respectively	[68]
N-carboxyethyl chitosan (CEC) Benzaldehyde-terminated Pluronic F127/carbon nanotubes (PF127/CNT)	▪ A bioadhesive with conductive, hemostatic, and self-healing properties ▪ Showed remarkable photothermal antibacterial property ▪ Exhibited a suitable gelation time, stable mechanical properties, hemostatic properties, high water absorbency, and good biodegradability ▪ Showed a pH-responsive release profile	▪ Mouse liver trauma ▪ Mouse liver incision ▪ Mouse-tail amputation	▪ Photothermal therapy of infected full-thickness skin wounds	▪ Showed an excellent treatment effect leading to significantly enhanced wound closure healing, collagen deposition, and angiogenesis in a mouse full-thickness skin wound-infected model	[69]

Material	Significant Characteristics of the Developed Hemostatic Sealant	Study Subject and Model	Application	Study Outcomes	Ref
Poly(lactic-co-glycolic acid) (PLGA) Poly(ethylene glycol) (PEG)	▪ A sprayable surgical sealant with high wet tissue adhesion, flexibility, biocompatibility, and hemostatic efficacy ▪ Deliverable directly to the site of surgery as fiber mats using solution blow spinning	▪ Rat liver	▪ Utility in procedures requiring simultaneous occlusion and hemostasis	▪ Produced intestinal burst pressures that were comparable to cyanoacrylate glue (160 mmHg) and ~3 times greater than fibrin glue (49 mmHg) ▪ Significantly decreased coagulation time *in vitro*	[74]
Gelatin-grafted-dopamine (GT-DA) Polydopamine-coated carbon nanotubes (CNT-PDA)	▪ A bio-inspired, bioactive, injectable composite hydrogel wound dressing with antioxidant and conductive properties ▪ Excellent photothermal effect and consequently antibacterial activity against Gram-positive and Gram-negative bacteria ▪ High biocompatibility	▪ Rat liver	▪ Wound dressing to promote the regeneration of infected skin and treat infected full-thickness defect wounds	▪ Excellent ability of these hydrogels to heal an infected full-thickness mouse skin defect wound	[75]
Fibrin agarose hydrogel	▪ A topical hemostatic agent with no haematoma and lower grades of haemorrhage, inflammation, and necrosis *in vivo*	▪ Rat liver	▪ A hemostatic agent in liver resection and likely in a range of surgical procedures	▪ Exhibited significantly higher hemostatic success rate (time to hemostasis) than other commercial haemostatic agents	[76]
Alginate and polyallylamine (PAA) coated with DOPA	▪ An injectable tissue adhesive with hemostatic ability ▪ Exhibits rapid hemostatic control	▪ Rat liver	▪ For treatment of hemorrhage caused by clinical procedures or trauma.	▪ Functional assay of Dopa-OA glue on hepatic bleeding animal model showed much enhanced hemostatic action	[77]

Material	Significant Characteristics of the Developed Hemostatic Sealant	Study Subject and Model	Application	Study Outcomes	Ref
Glycol chitosan-catechol hydrogel	▪ A bio-inspired hemostatic adhesive exhibiting negligible immune responses	▪ Rat liver	▪ A hemostatic adhesive agent with potential utility in various biomedical fields such as drug delivery and tissue engineering	▪ Significantly attenuated the immune response compared with chitosan-catechol	[78]
Serotonin conjugated hyaluronic acid	▪ A multifunctional hemostatic adhesive with a novel crosslinker and high biocompatibility	▪ Rat liver	▪ Surgical sealant of soft tissues ▪ Could be further expanded to tissue engineering scaffolds and drug delivery carriers	▪ Exhibited significantly improved hemostatic capability *in vivo* with normal and hemophilic injuries compared with a commercially available fibrin based hemostatic agent ▪ Prevented abnormal tissue adhesion after hemostasis	[60]
Oxidized bacterial cellulose (OBC) Chitosan (CS) with collagen (COL)	▪ A biodegradable antibacterial nanocomposite based hemostatic adhesive ▪ Exhibited rapid hemostasis and wound healing ▪ Possessed good mechanical strength, broad spectrum antimicrobial properties, and excellent biodegradability *in vivo*	▪ Rat liver	▪ Great potential for use as an absorbable hemostat for control of internal bleeding	▪ Exhibited better antibacterial properties, biodegradability, and biocompatibility than commercial absorbable hemostat product SURGUCEL® gauze ▪ Possessed greater procoagulant properties and blood clotting capability than SURGUCEL® gauze in a rat liver injury model	[79]

Material	Significant Characteristics of the Developed Hemostatic Sealant	Study Subject and Model	Application	Study Outcomes	Ref
Hyaluronic acid-graft-dopamine Reduced graphene oxide (rGO)	▪ An adhesive, hemostatic, and conductive injectable composite hydrogel with sustained drug release and photothermal antibacterial activity ▪ Exhibited high swelling, degradability, tunable rheological properties, and similar or superior mechanical properties to human skin ▪ Possessed sustained drug release capacity	▪ Mouse liver ▪ Mouse full-thickness wound repair model	▪ Full-thickness skin wound	▪ Significantly enhanced vascularization by upregulating growth factor expression of CD31 and improved the granulation tissue thickness and collagen deposition ▪ Exhibited higher therapeutic effect than the commercial Tegaderm films in a mouse full-thickness wounds model	[80]
Polysaccharide Oxidized carboxy-methyl cellulose A barbell-like peptide dendrimer based on generation 3 (G3) lysine and PEG (G3KP)	▪ A soft tissue bioadhesive with fast and high strength adhesion, antimicrobial, and hemostatic properties	▪ Rat liver	▪ Utility in diverse clinical applications of soft tissue sealing and repair	▪ Was shown to exhibit a 5-fold increase in adhesion strength compared to Coseal™ commercial bioadhesive ▪ Superior wound healing performance *in vivo* compared to Coseal™ and conventional sutures	[81]
Catechol-hydroxybutyl chitosan	▪ A thermoresponsive and injectable hemostatic adhesive with superior biocompatibility and biodegradability ▪ Exhibited excellent liquid-gel transition at different temperatures	▪ Rat liver	▪ Can be utilized for a wide range of biomedical applications	▪ Exhibited fast (within 30 s) in situ polymerization ▪ Effective hemostasis	[82]

Material	Significant Characteristics of the Developed Hemostatic Sealant	Study Subject and Model	Application	Study Outcomes	Ref
[Decanal] modified-Alaska pollock gelatin microparticles	▪ High tissue adhesiveness in wet conditions ▪ No undesirable adhesion to other tissues *in vivo* ▪ Promoted tissue regeneration	▪ Rat liver	▪ A wound dressing suitable for intra-/postoperative wounds	▪ Improved water/blood absorption and exerted hemostatic property in a rat model of liver injury ▪ Maintained tissue adhesiveness even after UV irradiation	[83]
Hydrocaffeic acid-modified chitosan Dodecyl aldehyde modified chitosan lactate	▪ A multifunctional biocompatible and bioadhesive hemostatic adhesive with anti-infective and pro-coagulant properties ▪ Possessed good antibacterial activity and anti-infection capability towards S. aureus and P. aeruginosa with no significant cytotoxicity ▪ Promoted wound healing	▪ Rat liver	▪ Surgical sealant for various soft tissues	▪ In situ antibleeding efficacy was demonstrated via the rat hemorrhaging liver and full-thickness wound closure models	[84]
Pentaerythritol tetraacrylate (PETEA) Poly(ethylene glycol) diacrylate (PEGDA-200) Dopamine	▪ An injectable and water-triggered bioadhesive exhibiting strong underwater adhesion and rapid sealing hemostasis ▪ Exhibited rapid and strong adhesion to diverse materials from low surface energy to high energy in various environments ▪ Capable of gluing dissimilar materials with distinct properties	▪ Rat Liver ▪ Rat femoral artery	▪ Visceral bleeding, especially hemorrhage from deep wound	▪ Could strongly adhere to diverse materials from low surface energy to high energy in deionized water, sea water, PBS, and a wide range of pH solutions (pH = 3 to 11) without use of any oxidant	[85]

Material	Significant Characteristics of the Developed Hemostatic Sealant	Study Subject and Model	Application	Study Outcomes	Ref
GelMA Hyaluronic Acid	▪ A photoreactive hydrogel with strong adhesive and hemostatic properties ▪ Could undergo rapid gelation and fixation to adhere to the target tissue	▪ Pig Carotid artery ▪ Pig heart	▪ For repair of arterial and heart bleeds	▪ Could withstand up to 290 mm Hg blood pressure in bleeding arteries (significantly higher than clinical systolic pressures of 60–160 mm Hg) ▪ Was shown to have stopped high-pressure bleeding from pig carotid arteries with 4~ 5 mm-long incision wounds and from pig hearts with 6 mm diameter cardiac penetration holes	[86]
Tannic acid Silk fibroin	▪ Exhibited tough adhesion and instant hemostatic ability in dynamic underwater environment	▪ Rat Liver ▪ Rat heart	▪ For sutureless sealing of ruptured tissues	▪ Exhibited tough adhesion to wet tissues (strength E134.1 kPa) even in the presence of blood and dynamic tissue motions (e.g., bleeding heart) ▪ Possessed instant hemostatic capability (within 30 s)	[66]
Aldehyde dextran (PDA)	▪ An in situ wet adhesive with rapid hemostasis ▪ Exhibited low cytotoxicity and hemolysis ▪ Could significantly accelerate coagulation by rapid wound block, fast cells aggregation and initiation, and high coagulation factors concentration	▪ Rabbit Liver ▪ Rabbit ear marginal veina ▪ Rabbit femoral artery	▪ Utility as quick-hemostatic dressing for uncontrollable hemorrhage	▪ The PDA sponge with pore size of ~30–50 μm fabricated by lyophilization exhibited fast blood absorption (47.7 g/g) ▪ Possessed strong tissue adhesion (~100 kPa) ▪ Achieved effective hemostasis and significant blood loss reduction in the ear vein, femoral artery, and liver injuries of rabbit models	[87]

3. Materials and Methods

3.1 Materials

Gelatin from porcine skin, methacrylic anhydride (MA), dopamine hydrochloride, (Benzotriazol-1-yloxy)tris(dimethylamino)phosphonium hexafluorophosphate (BOP), 1-Hydroxybenzotriazole hydrate (HOBt), Eosin Y disodium salt, Triethanolamine (TEA), N-Vinylcaprolactam (VC), hematoxylin-eosin y staining (H&E) solutions, Iron(III) chloride, and 3-(Trimethoxysilyl)propyl methacrylate (TMSPMA) were purchased from Sigma-Aldrich. Collagenase type II was purchased from Worthington Biochemical Co. Dulbecco's modified Eagle medium (DMEM) was purchased from Cellgro (Manassas, VA) and Fetal Bovine Serum (FBS) was obtained from HyClone (Logan, UT). 4',6-diamidino-2-phenylindole (DAPI) and live/dead viability kit were purchased from Invitrogen (San Diego, CA). SURGICEL® hemostatic gauze was purchased from Ethicon (Cincinnati, OH). Optimal Cutting Temperature (OCT) Compound was purchased from Sakura Finetek USA, Inc. (Torrance, CA).

3.2 Synthesis of GelMA

GelMA was synthesized as described previously [88, 89]. Briefly, gelatin from porcine skin (10 g) was dissolved in DPBS at 50 °C. 8 %(v/v) methacrylic anhydride (MA) was added dropwise under continuous stirring at 50 °C. After 3 h, the solution was diluted with DPBS to stop the reaction. The diluted solution was dialyzed against DI water at 50 °C for 5 days. The resulting solution was then filtered under sterile conditions, frozen at – 80 °C overnight, and lyophilized for 5 days.

3.3 Synthesis of GelMAC

800 ml of deionized (DI) water was bobbled with nitrogen gas for 30 minutes to remove air from the DI water. Gelatin was added at a final concentration of 4 mg/ml to water at 50°C. 2 mM of BOP ((benzotriazol-1-yloxy)tris(dimethylamino)phosphonium hexafluorophosphate), 2 mM of HOBt (1- hydroxybenzotriazole), 20 mM of dopamine hydrochloride, and 20 mM of triethylamine were then added. The reaction mixture was continuously stirred with a stir bar for 2 hr under N_2 atmosphere. The dopylated gelatin was precipitated with cold acetone. The resulting dopylated gelatin was then metacrylated utilizing methacrylic anhydride as previously described. Briefly, dopylated gelatin was dissolved in PBS at a concentration of 10% (w/v) and heated at 50°C for 20 minutes. Dropwise addition of 8% (v/v) methacrylic anhydride under continuous stirring at 50°C, followed by dilution after 2 hours with PBS and finally, dialysis against deionized water at 40-50°C for 5 days. After sterile filtration and lyophilization for 5 days, GelMAC prepolymer was stored at 4C until experimental use.

To form the GelMAC hydrogel system, a two-step crosslinking system was utilized. In the first crosslinking step, different concentrations of Fe^{3+} ions (0, 1, 2.5, 5 and 10 μM) were introduced to a 20 %(w/v) GelMAC prepolymer solution to form Fe^{3+}-mediated coordinative noncovalent crosslinking network. For the second crosslinking step, the prepolymer solution was irradiated with an FDA-approved FocalSeal visible light source (Genzyme Biosurgery, Inc., 450-550 nm) for 4 minutes to facilitate the formation of covalent bonds between the MA groups. The prepolymer solution contained 0.1 mM Eosin Y, 1 %(w/v) N-vinylcaprolactam (VC), and 1.5 %(w/v) triethanolamine (TEA), as type 2 initiator, co-monomer, and co-initiator, respectively.

3.4 Hydrogel Preparation

The lyophilized GelMA/GelMAC prepolymer was dissolved in a solution containing TEA and VC in DPBS. Iron chloride solution at various iron concentrations (i.e., 0, 1, 2.5, 5, 10 μM) were prepared and stored in 4°C prior to use. Eosin Y disodium salt was dissolved separately in DPBS and was then added to the prepolymer/Fe/TEA/VC solution to form the final precursor. The final concentration of each component in the mixture is as follows: 20% prepolymer, 1.875 %(w/v) TEA, 1.25% (w/v) VC, 0.1 mM Eosin Y, and various concentrations of Fe (i.e., 0, 1, 2.5, 5, 10 μM). To form the hydrogels, 70 μl of the mixture was pipetted into polydimethylsiloxane (PDMS) cylindrical molds (diameter: 6 mm; height: 2.5 mm) for compressive tests, or rectangular molds (12.5 × 4.5 × 1.25 mm) for tensile test. The solutions were then photopolymerized via exposure to visible light (Genzyme Biosurgery, Inc., 450-550 nm) for 4 minutes.

3.5 Evaluation of *in Vitro* Swelling Ratio

The swellability of GelMA/GelMAC hydrogels was defined by calculating the ratio of weight change at each timepoint to the initial weight of the hydrogel. For this, hydrogels were formed as described in previous section and weighed (initial weight) following by submerging them into DPBS at 37 °C. Excess buffer was gently removed using a disposable wipe, and the wet weight of the hydrogels were measured at different time points for up to 48 h.

3.6 Evaluation of *in Vitro* Enzymatic Degradation

To evaluate the percentage of *in vitro* degradation, GelMA/GelMAC hydrogels were weighed immediately after crosslinking, and placed in separate wells of a 24 well plate. Each well was filled with 1 ml of DPBS containing 20 μg/ml collagenase type II and kept at 37

ºC. The enzyme-containing DPBS solutions were changed every 2 days during this experiment for 3 weeks. The samples were then freeze-dried and weighed on days 1, 4, 7, 10, 12, 16, 20 and 24 post-incubation (n = 4). The percentage degradation of the gels was determined using Equation (1).

$$\text{Degradation (\%)} = \frac{W_0 - W_t}{W_0} \times 100 \quad (1)$$

Where, W_0 is the initial sample dry weight and W_t is the dry weight after time t.

3.7 *In Vitro* Burst Pressure

The burst pressure of the GelMAC and GelMA hydrogels were measured based on the ASTM testing standard (ASTM F2392-04). Collagen sheet was cut to a dimension of 40 mm× 40 mm. Next, the porcine intestine was placed between two stainless steel plates (35 mm× 35 mm), in which the upper piece had a 10-mm-diameter hole in its center and a circular defect (2 mm in diameter) was created on the center of the porcine intestine. 20 µl of the adhesives were injected over the defect and exposed to visible light. Next, the porcine intestine was placed into the burst pressure testing system, consisting of a pressure sensor, a recording unit. Air was then supplied using a syringe pump at a rate of 5 ml/s to the sample until bursting ($n \geq 5$).

3.8 *In Vitro* Wound Closure

The adhesion strength of the GelMAC and GelMA hydrogels was evaluated according to a modified ASTM testing standard (ASTM F2458-05). Briefly, fresh porcine skin or porcine lung was obtained from a local slaughterhouse and were cut into rectangular sections (10 mm × 30 mm). The porcine skin or porcine lung was kept moist with DPBS prior to use. The tissues were fixed

onto two precut glass slides (30 mm × 60 mm) using Krazy Glue. The tissue was then cut from the middle with a single edge cutter blade. Afterwards, 40 µl of the precursor solution was pipetted onto the tissue interface and subsequently crosslinked with visible light.

3.9 Blood Clotting Assay

A volume of 630 µL freshly-extracted blood was pipetted into a 1.5 mL Eppendorf tube. A total of 70 µL of 0.1 M calcium chloride ($CaCl_2$) was then added, followed by vortexing for 10 s. Then, 100 µL was deposited into sequential wells on a 48 well plate. At selected time points, each well was washed with 9 g/L saline solution to halt clotting. The liquid was immediately aspirated, and washes were repeated until the solution was clear, indicating removal of all soluble blood components. In case of the GelMAC and GelMA experimental groups, the prepolymer solution were pipetted at the base of the well plates, ensuring the entire bottom surface was coated with gel and then photocrosslinked. After a trial was complete, the final clotting time was marked in the well that formed a uniform clot, with no change in clot size in subsequent wells.

3.10 Liver Bleeding Model

All animal experiments were approved by the UCLA Animal Research Committee (UCLA ARC #2017-096-01). The animal experiments were conducted in accordance with the relevant guidelines. A set of 6 experimental groups were selected for this study which included the no treatment group (injury only) as negative control, the GelMA hydrogel with or without ferric ion, the GelMAC hydrogel with or without ferric ions, and the commercial absorbable hemostatic agent, SURGICEL® (Ethicon, Cincinnati, OH, USA) to serve as positive control groups. Under general anesthesia (1.5% isoflurane in 100% O2), median laparotomy was conducted, a wound

retractor was placed, and the operating field around the liver was draped with filter paper to collect the whole amount of blood from the incision site. A standardized liver wound was made using 2mm-sized biopsy punch. Immediately, a hemostatic hydrogel was applied to the bleeding lesion and crosslinked for 2 minutes using visible light. The amount of blood absorbed to the filter paper was measured. Afterwards, the abdominal wound was anatomically closed using 4-0 absorbable sutures and 4-0 non-absorbable sutures/staples by closing the peritoneum and the abdominal skin separately. The relative bleeding amount was calculated using the following formula. (Sample blood absorbing filter paper weight -filter paper weight)/Average value of blood absorbing filter paper weight in the Injury only group. The animals were weighed and monitored daily for signs of pain or discomfort.

3.11 Data Analysis

Data analysis was carried out using a 1- or 2-way ANOVA test with GraphPad Prism 6.0 software. Error bars represent mean ± standard deviation (SD) of measurements (*$p < 0.05$, **$p < 0.01$, ***$p < 0.001$, and ****$p<0.0001$).

4. Results and Discussions

GelMAC and GelMA hydrogels were synthesized and prepared as described in the "Materials and Methods" section. Various concentrations of the Fe^{3+} ions have been incorporated to optimize and characterize the effect of the metal ions on the properties of the developed hydrogels. In all experiments conducted, GelMA hydrogels have been tested to serve as positive control with the exception of *in vitro* blood clotting assay and *in vivo* liver bleeding experiment. Upon

characterization of chemical, mechanical, swelling, and degradation profiles of the developed hydrogels, the optimized formulation of GelMAC and GelMA hydrogels containing 2.5μm Fe^{3+} ion concentration was selected and utilized for further experimentation. These hydrogel formulations are referred to as "GelMAC-Fe" and "GelMA-Fe" there on.

4.1 Synthesis and Chemical Characterization

The chemical modification of gelatin backbone through conjugation of dopamine followed by conjugation of methacrylate group is shown in Figure 4.1A. The schematic representation also illustrates the preparation of the GelMAC prepolymer solution and its application and polymerization at the defect site on the tissue surface. Utilizing a naturally derived biomolecule as the polymer backbone, gelatin (denatured collagen), ensures the biocompatibility and biodegradability of the resulting hydrogel. In addition, gelatin offers numerous essential functionalities through its amino acid building blocks having hydroxyl (-OH), amine (NH_2), and carboxylic acid (COOH) groups [90]. Employing these abundant chemical functionalities of gelatin macromolecules, allows to chemically conjugate both methacrylic anhydride and dopamine molecules to the gelatin backbone. In this project, the dopamine molecules were first covalently conjugated with existing carboxylic acid groups on the gelatin backbone through the formation of amide bonds. In the second step, methacrylate (MA) groups were covalently linked with the amine residue of gelatin biomacromolecule. These chemical modifications enabled both photo- and chemical crosslinking of the gelatin biopolymer. To form the GelMAC hydrogel system, the prepolymer solution was mixed with Fe^{3+} ions introducing noncovalent interaction between the catechol groups through the chelation mechanism. In addition, the applied prepolymer solution was irradiated with visible light to facilitate the formation of covalent bonds between the MA

groups. Incorporation of such sequential inter- and intramolecular covalent and noncovalent interactions eventually results into the formation of a dual crosslinked hydrogel matrix. In addition, structurally, due to the presence of multiple functional groups, the hydrogel matrix contains various chemical interactions. This includes π- π interaction (between aromatic groups, catechol), chelation complex (between Fe^{3+} and catechol), hydrogen bonding (between hydrophilic groups like -OH, -COOH, and $-NH_2$) and C-C covalent bond (between MA) formation and are presented in Figure 4.1A. Specific contribution of this MA-functionality towards tissue adhesion upon photocrosslinking was demonstrated in a recent work over different biological surfaces [91]. MA groups also initiate Michael addition reaction with the functional groups present over the tissue surface during the photocrosslinking process.

Successful chemical conjugation of dopamine molecules was confirmed with Fourier-transform infrared spectroscopy (FTIR). Figure 4.1B compares the FTIR spectra of GelMAC and gelatin polymers where the structural and functional difference between these two biopolymers was due to the presence of the peaks corresponding to the catechol motifs of dopamine molecule. For example, the peak observed around 1000 cm^{-1} in GelMAC spectrum corresponded to the aromatic C-H bending of the catechol moieties [92, 93]. Similarly, the peak at 1550 cm^{-1} was related to the aromatic C-C stretching of chemically attached dopamine molecules [93]. Chemical modification of gelatin with methacrylic anhydride was further confirmed via proton nuclear magnetic resonance (^{1}H-NMR) analysis on GelMA and GelMAC polymers (Figure 4.1D). In both cases, appearance of vinyl C-H peaks at δ=5.3 ppm (peak b) and 5.6 ppm (peak a) confirmed the covalent linkage of MA groups with gelatin biomacromolecules [88]. Degree of conjugation of MA groups to the gelatin backbone for GelMA and GelMAC polymers was calculated to be ~55% and ~40%, respectively. This observed difference be explained with the steric effect due to the presence of

covalently linked dopamine molecules on the GelMAC macromolecules. Moreover, GelMAC prepolymer solution was found to exhibit higher viscosity compared to the GelMA as shown in Figure 4.1C. This is associated with the existence of additional catechol moieties which possess π- π interaction with the free π electrons. Also, these catechol moieties can readily interact with π electrons of the MA groups (Figure 4.1A) and even with the Fe^{3+} ions [94] leading to significant change in the physio-chemical properties of GelMAC prepolymer solution. Such intra- and intermolecular interactions are studied and found to enhance the cohesive interactions [94].

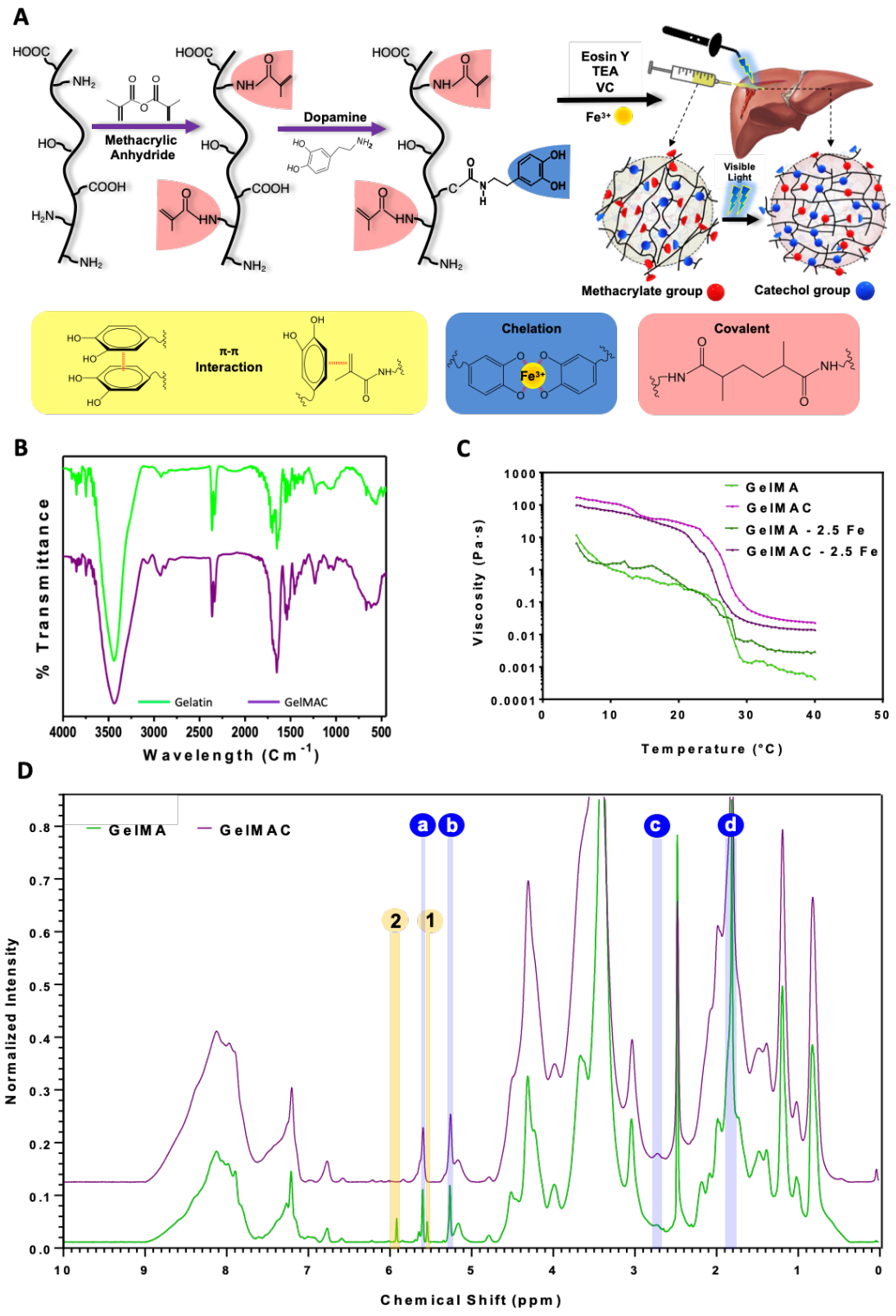

Figure 4.1 Synthesis and chemical characterization of GelMA and GelMAC prepolymers. A) Schematic illustration of the process for the GelMAC synthesis and the use of the adhesive hydrogels for liver as hemostatic sealant. **B)** Representative FTIR spectra of gelatin and GelMAC prepolymer. **C)** Representative viscosity curves for GelMA, GelMAC, GelMA-Fe, and GelMAC-Fe before photo-crosslinking. **D)** ^{1}H-NMR spectra on GelMA and GelMAC polymers.

4.2 Mechanical Characterization

GelMA-based adhesives have been demonstrated to possess optimal mechanical and adhesive properties as tissue sealant or bioadhesive. In addition, the mechanical properties of the developed GelMAC hydrogels are highly tunable due to the ability to optimize the concentrations of Fe^{3+} ions in the hydrogel matrix. This high tunability therefore can provide the ability to best mimic the mechanical properties of the native tissue closely. Therefore, the mechanical properties of both GelMA and GelMAC formed by using different concentrations of Fe^{3+} ion ($FeCl_3$) were characterized. Here, both GelMAC and GelMA prepolymer solutions were mixed with Fe^{3+} ions and photocrosslinked with visible light for 240 sec before the tests were conducted. According to the results obtained, the elastic moduli for both GelMAC and GelMA hydrogels (20% w/v) were increased upon introducing the Fe^{3+} ions (Figure 4.2A). For instance, GelMAC hydrogels containing 2.5 and 5.0 μM of Fe^{3+} (i.e., 202.7 ± 28.4 and 194.1 ± 16.9 kPa, respectively) exhibited higher elastic modulus than the GelMAC hydrogel without Fe^{3+} ions (i.e., 168.7 ± 11.7) (Figure 4.2A). This is due to the formation of catechol-Fe^{+3} complexes (mono- and bis- catechol-Fe^{3+} complexes) at normal pH of 7.4 [95]. Similar effect was also observed for GelMA hydrogels where instead of the catechol groups, Fe^{+3} ions could interact with the carboxylic acid groups on the gelatin backbone [96] and effect the mechanical properties of the resulting hydrogel by reorganizing the gelatin network. For example, elastic modulus of the GelMA hydrogel containing 2.5 and 5.0 μM of Fe^{3+} was 302.3 ± 9.3 and 246.6 ± 45.2 kPa, respectively, whereas GelMA hydrogel without Fe^{3+} showed a value of 257.0 ± 28.7 kPa. Interestingly, in general, mechanical strength of the GelMA hydrogels were observed to be higher compared to the GelMAC hydrogels across all Fe^{3+} concentrations. This observation is due to the existence of the additional secondary crosslinking mechanism of the catechol moieties and the Fe^{3+} ions. This consequently resulted in

an interruption of the photocrosslinking of methacrylate groups, the primary source of mechanical strength of the hydrogels, in presence of aromatic groups. Typically, aromatic groups with π-electron cloud (dopamine) readily interact with the C=C group (methacrylate groups) and consequently restrict the involvement of C=C during photocrosslinking. In addition, because of these π-π interactions, molecular movements of the GelMAC polymers are reduced. As a direct result of these two types of interactions, a fewer number of methacrylate groups are crosslinked. On the other hand, the covalent bonding of methacrylate groups is responsible for observed higher mechanical strengths in photocrosslinked hydrogels.

Moreover, high absorption intensity of catechol-Fe^{3+} complexes (at around 350-470 nm) interferes with the photocrosslinking process [97]. It was also observed that the mechanical properties of the hydrogels decreased by increasing the Fe^{3+} ion concentrations to 10 μM. This drop in elastic modulus at 10 μM Fe3+ ion concentration could be due to the higher acidic condition, which disturbed the hydrogen bonding in GelMA and GelMAC hydrogels. Similar trends were observed in compressive modulus of the GelMAC and GelMA hydrogels formed by varying the Fe^{3+} ion concentrations (Figure 4.2B), demonstrating the highest compressive modulus at 2.5 μM Fe^{3+} ion concentration. Cohesion interaction forces inside the 3D hydrogel network were demonstrated with the ultimate stress values of the hydrogels at various Fe^{3+} ion concentrations (Figure 4.2C). Maximum ultimate stress values for GelMA and GelMAC hydrogels (at 2.5μm Fe^{3+} ion concentration) were found to be 119.1 ± 7.3 and 88.42 ± 19.9 kPa, respectively. In addition, the extensibility (ultimate strain) of GelMA and GelMAC hydrogels across all Fe^{3+} ion concentrations demonstrated similar results, with recorded stretchabilities in the order of 32-41 % (Figure 4.2D). The developed GelMAC hydrogel (across all Fe^{3+} ion concentrations) exhibited similar elasticity to soft tissues such as lung (~40% elasticity [98, 99]), and therefore possess the mechanical

characteristics of a suitable candidate for such applications. Moreover, among the various formulations of GelMAC hydrogel with ferric ions, GelMAC hydrogel with 2.5µm Fe^{3+} ion concentration exhibited the highest ultimate strength (88.42 ± 19.9 kPa). Therefore, it is expected that this formulation can withstand the physiomechancial forces exerted on a soft tissue wound site. The optimized mechanical properties of the GelMAC hydrogels have shown that the GelMAC hydrogel with 2.5µm Fe^{3+} ion concentration can therefore allow normal tissue function without compromising the tissue movement.

4.3 Assessment of the Swellability and Degradation Rate

In order to assess the stability of the engineered hydrogels against swelling and degradation in physiological environments, *in vitro* swelling and degradation studies were carried out. The *in vitro* swellability of the GelMAC and GelMA hydrogels in DPBS at 37°C was measured over 48 hours duration (Figure A-1A,B). According to the results of this study, higher swelling ratio was observed for GelMAC hydrogels as compared to GelMA hydrogels across all Fe^{3+} ion concentrations. This could be attributed to the presence of catechol-Fe^{+3} coordination bonds providing dynamic and spatially reconfigurable interactions [9, 100-102]. Moreover, the lower degree of crosslinking as well as the presence of hydrophilic groups in the GelMAC hydrogel is responsible for the observed higher swelling ratio compared to the GelMA hydrogels. While incorporation of dopamine molecules having polar -OH groups enhance the water diffusion through the increase in water-polymer (GelMAC) interactions, it reduces the crosslinking within the networks making it a soft hydrogel material. For example, while GelMAC hydrogel with 2.5 µM Fe^{3+} showed a maximum swelling ratio of 44.9 ± 6.7 %, GelMA hydrogel incorporating the same Fe^{3+} ion concentration reached a maximum swelling ratio of 14.3 ± 4.3 % (Figure 4.2E). However, rate of swelling of the hydrogel was observed to be lower for GelMAC hydrogel. For

example, while GelMAC hydrogel with 2.5 μM Fe^{3+} showed a maximum swelling after 8 h, GelMA hydrogel incorporating the same Fe^{3+} ion concentration reached a maximum swelling within 4 h. This is due to the presence of non-polar π- π interaction (Figure 4.1A) in the GelMAC hydrogel. Further studies on the swelling of GelMA and GelMAC hydrogels with various concentrations of Fe^{+3} ion showed significant increase in swelling ratio at high Fe^{+3} ion concentration (10 μM) compared to others (bellow 10 μM) (Figure A-1A,B). This can be due to the change in the pH value of the hydrogel arising from the high Fe^{3+}ion concentration, resulting into the interruption of the formation of a homogeneous hydrogel structure. Meanwhile, this affect was also reflected in the elastic and compressive modulus values obtained for hydrogels formed at high Fe^{+3} ion concentration (Figure 4.2A,B). The *in vitro* degradation rates of the hydrogels were studied by incubation in DPBS containing collagenase type II (20 μg/ml) over 21 days (Figure A-1C,D). Although the swelling ratio of the GelMAC hydrogel was higher compared to the GelMA hydrogel, both GelMA and GelMAC hydrogels containing 2.5 μM Fe^{3+} ion exhibited similar weight loss profile with time (Figure 4.2F). In addition, similar rates of degradation were observed for both GelMA and GelMAC hydrogels which completely degraded after 21 days of incubation (Figure 4.2F). These results also demonstrate that the *in vitro* enzymatic degradation of the hydrogels was independent of the Fe^{3+} ion concentrations (Figure A-1C,D). Therefore, the biodegradability profile of the newly developed GelMAC hydrogel was remained unaltered. Moreover, these result further confirm that despite exhibiting lower degree of photocrosslinking than GelMA, GelMAC hydrogels can sustain their stability in physiologically relevant enzymatic environment due to their enhanced functional interactions.

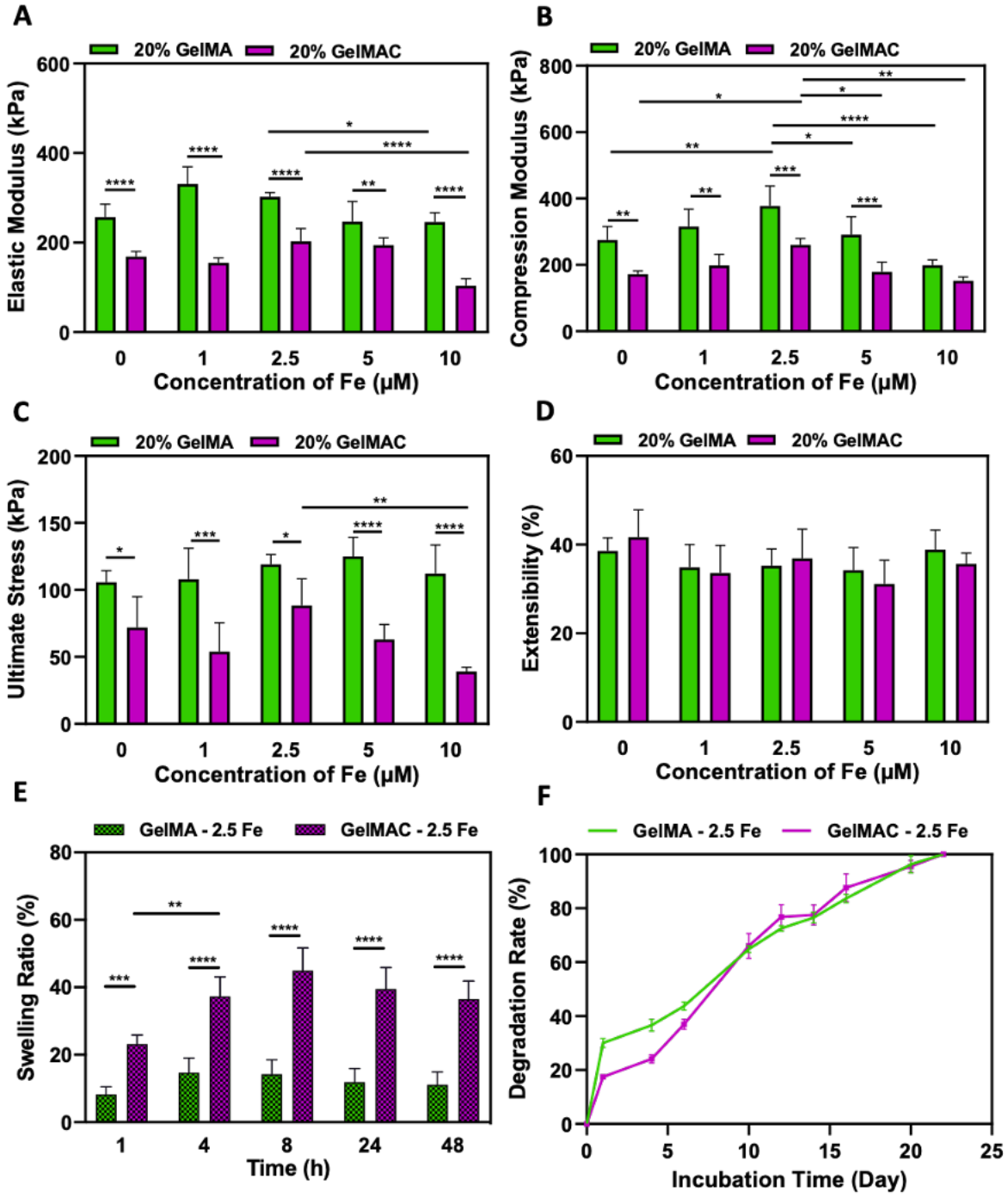

Figure 4.2 Mechanical characterization, swellability and degradation rate of GelMA and GelMAC hydrogels. **A)** Elastic modulus, **B)** Compressive modulus, **C)** Ultimate stress, and **D)** Extensibility, of hydrogels containing various concentrations of ferric ions (Fe^{3+}). Data are represented as mean ± SD (*$p < 0.05$, **$p < 0.01$, ***$p < 0.001$ and ****$p < 0.0001$, $n \geq 6$). **E)** Swelling ratio of hydrogels containing 2.5 μM concentrations of ferric ions (Fe^{3+}) in DPBS. **F)** Degradation rate of hydrogels containing 2.5 μM concentrations of ferric ions (Fe^{3+}) in enzyme-containing DPBS solutions. Data are represented as mean ± SD (**$p < 0.01$, ***$p < 0.001$ and ****$p < 0.0001$, $n \geq 4$).

4.4 Characterization of the Adhesive Properties

Incorporation of catechol moieties to the gelatin polymer backbone was observed to improve the adhesive properties of the resulting hydrogel. To evaluate adhesive properties of the GelMAC, *in vitro* standard wound closure test using porcine lung and skin tissues as well as burst pressure tests were performed and compared with GelMA as control. It is known that catechol functionalities strongly interact with biological surfaces having hydrophilic groups such as amines, acids, hydroxyl groups and others [39]. Such interactions include both hydrogen bonding and covalent attachment. Figure 4.3A represents the potentially feasible chemical interactions between tissue surfaces and our developed GelMA bioadhesives upon photocrosslinking. Figure 4.3A-i shows the active chemical interactions related to GelMA hydrogels having MA groups whereas chemical interactions associated with GelMAC hydrogels having both MA and catechol groups is presented in Figure 4.3A-i and ii. Here, Figure 4.3A-ii illustrates the contribution of catechol groups, alone. The experimental set up is shown in Figure 4.3A-iii.

In vitro wound closure tests performed with GelMAC and GelMA hydrogels using porcine lung tissues (Figure 4.3B) and porcine skin tissues (Figure 4.3C) as biological tissue models. Although GelMAC hydrogels exhibited slightly lower mechanical properties compared to the GelMA hydrogels (Figure 4.2A,B), the tissue adhesive strength of GelMAC hydrogels were observed to be significantly higher than GelMA hydrogels. For example, GelMAC hydrogels containing 1 and 2.5 μM Fe^{+3} ion concentrations exhibited adhesive strengths of 37.1 ± 4.5 and 33.7 ± 3.8 kPa, respectively, to the porcine lung tissue (Figure 4.3B). Whereas for GelMA hydrogels, these values were in the range of 17-24 kPa for all the Fe^{+3} ion concentrations (Figure 4.3B). Such enhancement in the adhesion strength of GelMAC to the lung tissue attributed to the presence of catechol groups on GelMAC which facilitated the formation of various covalent or physical bonds with lung tissue

surface, described in Figure 4.3A-i and ii. These interactions include hydrogen bonding (between the catechol moieties and quinone functionalities of the polymer and the hydroxyl group of the tissue), Schiff base (between the quinone functionality of the polymer and the amine group of the tissue), and Michael addition (between the dopamine molecule of the polymer and the amine or thiol group of the tissue). Similarly, GelMAC hydrogels formed with various Fe^{3+} ion concentrations showed superior adhesion on the porcine skin tissue compared to the GelMA hydrogels (Figure 4.3C). For instance, GelMAC hydrogel formed with 2.5 μM Fe^{3+} had an adhesion strength of 32.9 ± 7.2 kPa, which was significantly higher than GelMA hydrogel with adhesion strength in the range of 13.9-15.9 kPa. However, initial decrease in the adhesion strength (at 1 μM Fe^{3+}) immediately following the incorporation of Fe^{3+} ions, for both GelMAC and GelMA hydrogels is related to the facile complexation of Fe^{3+} ions with carboxylic acid groups present in the polymer backbone. This eventually enhances the cohesion interactions through the formation of ionic bonds [96], rather than the adhesive interaction with tissue surface as observed in Figure 4.2A,B.

The adhesive strengths of the developed hydrogel were further characterized with burst pressure test using collagen sheet which resembles biological superstrate such as porcine intestine (Figure 4.3D). Figure 4.3E shows the burst pressures of GelMAC and GelMA hydrogels formed by using various concentrations of Fe^{3+} ions. The burst pressure vales for GelMAC hydrogels containing 2.5 and 5 μM of Fe^{3+} ions were 34.0 ± 1.0 and 44.8 ± 3.1 kPa, respectively. These values are significantly higher than the corresponding values for GelMA formed by using 2.5 μM Fe^{3+} ions (19.8 ± 5.9 kPa) and 5 μM of Fe^{3+} ions (21.2 ± 4.8 kPa). In addition, improved burst pressure values were observed for GelMAC hydrogel (21.8 ± 2.0 kPa) as compared to GelMA hydrogel (28.8 ± 11.2 kPa) formed without Fe^{3+} ions. This highlights the contribution of catechol

functionalities in improving the adhesion strength of the bioadhesives. The high adhesion of the GelMAC to different tissue surfaces, through the catechol-tissue interactions, highlights the potential of the synthesized bioadhesives to be used to seal wounds *in vivo*. Due to the high adhesiveness and mechanical properties of the GelMAC bioadhesive containing 2.5 μM of Fe^{3+} ion concentration, this formulation was selected for further studies. This was named as GelMAC-Fe and compared with GelMA-Fe as a reference.

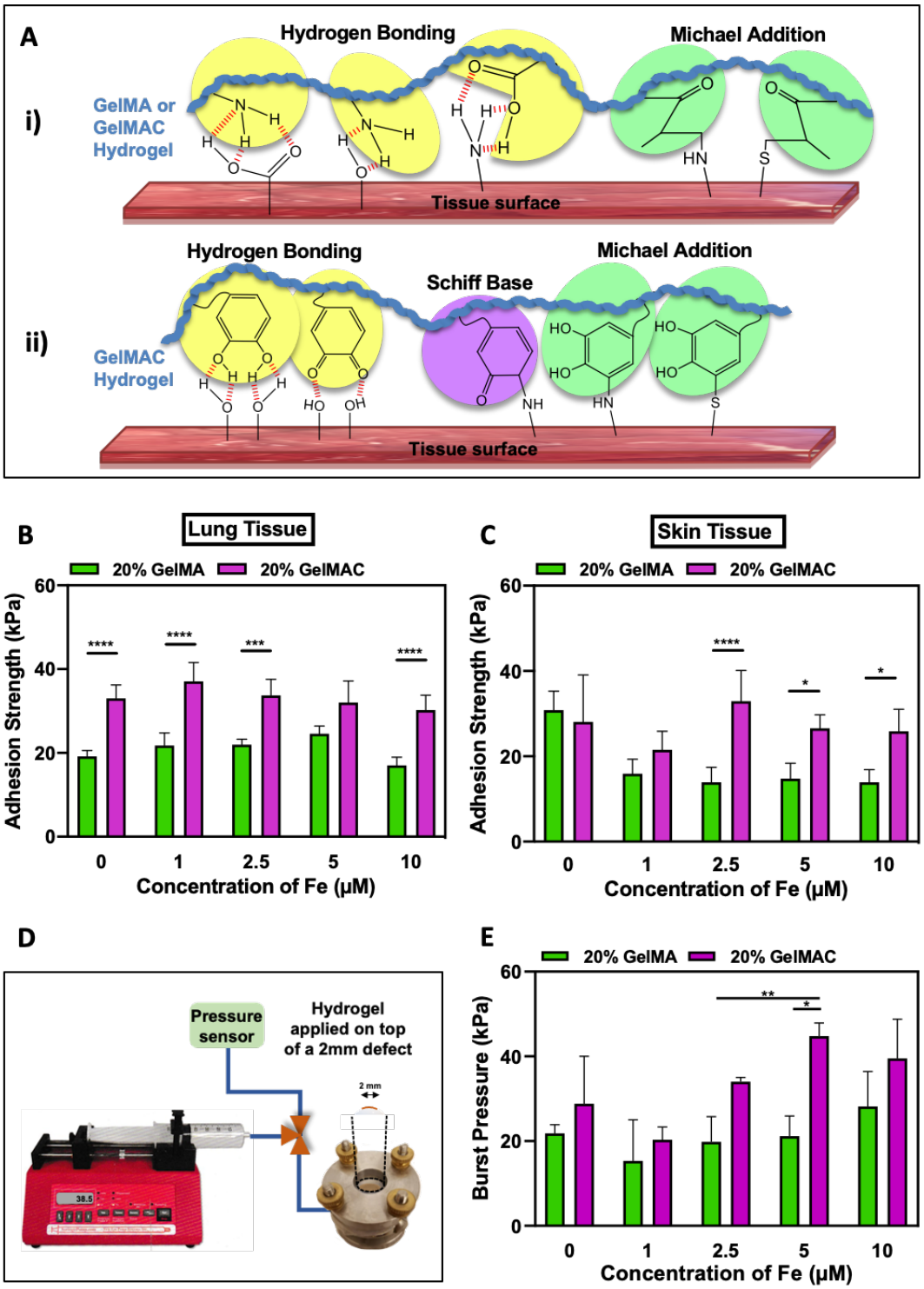

Figure 4.3 Adhesive properties of the GelMA and GelMAC hydrogels. A) A schematic of the potential molecular interactions between hydrogels and tissue. **B)** *In vitro* adhesion strength of hydrogels containing various concentrations of ferric ions (Fe^{3+}) using porcine lung tissue and **C)** Porcine skin tissue. **D)** An illustration of burst pressure measurement setup. **E)** *In vitro* burst pressure measurements of hydrogels containing various concentrations of ferric ions (Fe^{3+}) using collagen sheet. Data are represented as mean ± SD (*$p < 0.05$, **$p < 0.01$, ***$p < 0.001$ and ****$p < 0.0001$, $n \geq 6$).

4.5 Assessment of the *In Vitro* Clotting Time

The control of bleeding from the wound site especially during surgery is highly desired. Hemostatic materials employing different blood coagulation mechanisms have emerged and are widely used to control the bleeding in various clinical settings and combat environments [3]. Such blood coagulation mechanisms include the absorption of blood fluid, incorporation of clotting factors, or sealing the wound area to stop the bleeding. Hemostatic sealants offer a great advantage to their counterparts in their ability to control the bleeding, as their efficacy of blood coagulation is independent of the clotting cascade (which can be already compromised in patients with certain blood coagulation abnormalities). Due to the observed high adhesion strength of GelMAC hydrogels as well as the incorporation of the ferric ions, their hemostatic ability was evaluated by monitoring the clotting time of whole human blood placed in direct contact with the photocrosslinked hydrogel adhesives (Figure 4.4A). Blood clotting times were calculated for six test groups including whole blood (negative control), GelMA, GelMA-Fe, GelMAC, GelMAC-Fe, and clinically utilized commercial hemostatic product, SURGICEL® (Figure 4.4B). Interestingly, blood coagulation time for the GelMA hydrogel (without any Fe^{3+} ions) was observed to be 14.3 ± 0.6 min, exhibiting no significant difference when compared to the control group (whole blood in the wells), which formed blood clot within 15.7 ± 0.6 min. In contrast, GelMAC hydrogel (without any Fe^{3+}) significantly reduced the blood clotting time to 11 ± 1 min, promoting hemostasis. This observation could be due to the presence of catechol moieties on the polymer backbone which assisted in the interactions with serum proteins and other blood cells (i.e., erythrocytes, white blood cells, or platelets) [103, 104]. Meanwhile, both GelMA-Fe and GelMAC-Fe hydrogels were observed to have improved hemostatic abilities (Figure 4.4A,B). For instance, the clotting time corresponding to the GelMA-Fe and GelMAC-Fe were 9.7 ± 0.6 min

and 9.3 ± 0.6 min, respectively. This is comparable to the commercial hemostatic sealant, SURGICEL® with recorded blood coagulation time within 8.7 ± 0.6 min under the same experimental conditions. Chemically, Fe^{3+} ions readily interact with blood proteins through the extended electrostatic and hydrogen bonding interactions [105] and therefore, can act as a blood coagulating agent. In addition, catechol functionality and its partially oxidized form together [104] play a synergistic effect to significantly reduce the clotting time for GelMAC-Fe hydrogel (Figure 4.4A,B). Enhanced hemostatic activities of the engineered hemostatic bioadhesives was further characterized with absorbance and clot weight measurements. In order to quantify the evaluation of the coagulation process, the commonly used UV-visible absorbance (405 nm) detection by a micro-plate reader was employed [106]. A clotting time assay was performed in which wells of a 96-well plate were used to monitor the progression of clot formation. Figure 4.4C describes the absorbance values of corresponding samples at different time points. Briefly, following treating the whole blood with the engineered hemostatic bioadhesives and SURGICEL® for 7, 12, 16, and 20 min, the wells were washed with DPBS and the absorbance in each well was measured at λ_{ab} = 405 nm. No significant change was observed in the absorbance for all experimental groups at 16 min and 20 min time points, confirming the completion of the blood coagulation process (Figure 4.4C). In addition, the higher absorbance values for the GelMAC-Fe when compared to SURGICEL®, confirmed the better hemostatic activity of GelMAC-Fe. Similarly, the weight of the collected blood clot associated with the GelMAC-Fe hydrogel at 16min time point was observed to be higher than GelMAC and GelMA hydrogels, as well as SURGICEL® (Figure 4.4D). This clearly showed the synergistic effect of the Fe^{3+} ions and the catechol groups in the GelMAC-Fe hydrogel towards the development of a hemostatic sealant.

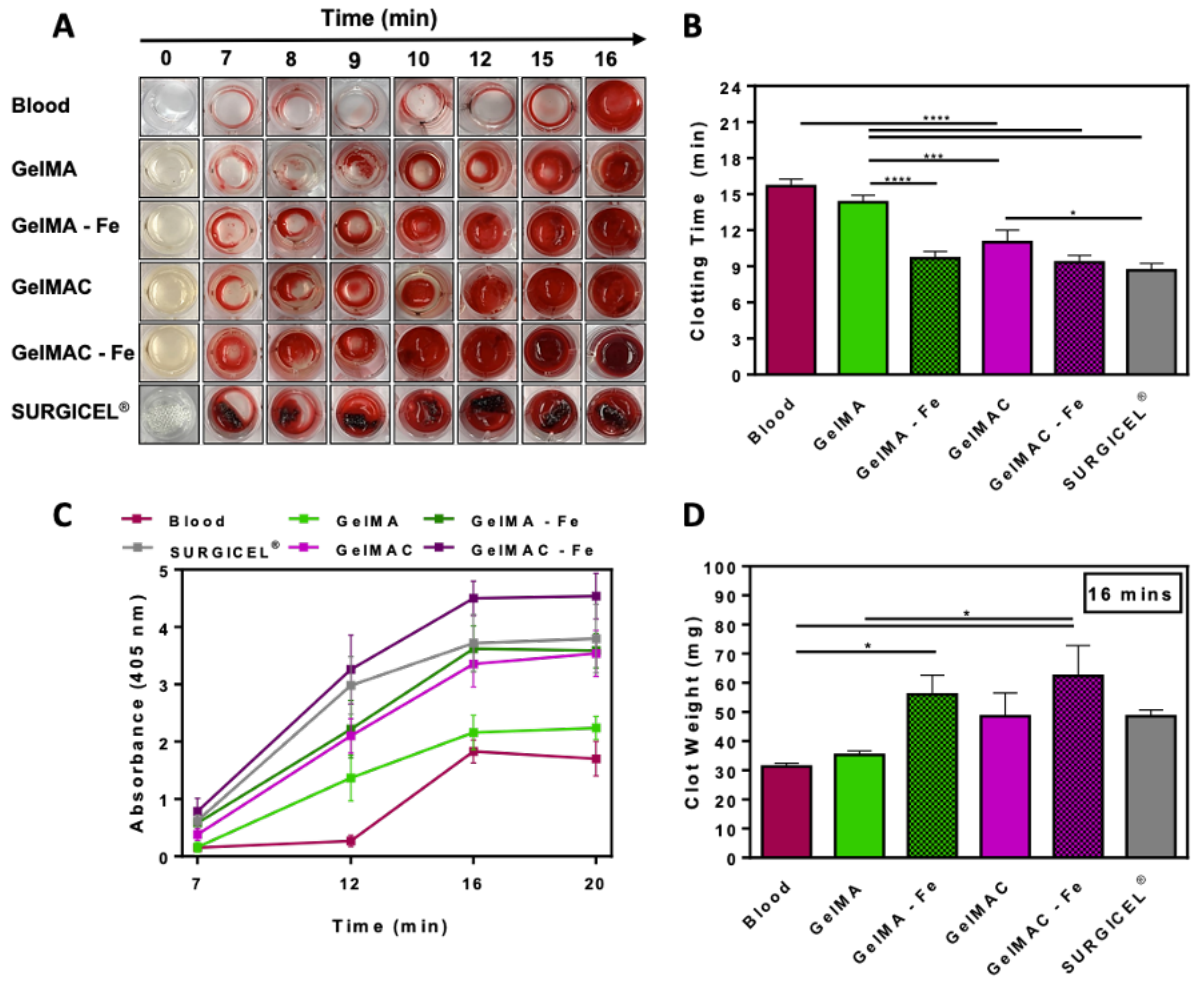

Figure 4.4 Effect of hydrogels and iron (Fe) on clotting time. A) Time-dependent clot formation of GelMA, GelMAC, GelMA-Fe, and GelMAC-Fe hydrogels compared with untreated blood (negative control) and SURGICEL® absorbable hemostat (positive control). **B)** Quantitative clot formation time. **C)** Absorbance at 405nm wavelength performed on clotted samples at various time points of 7, 12, 16, and 20 minutes. **D)** Clot weight collected at 16 minutes time point. Data are represented as mean ± SD (*p<0.05, ***p<0.001, ****p<0.0001 and n=4).

4.6 Assessment of the *In Vivo* Hemostatic Efficacy

Due to the observed *in vitro* hemostatic ability of the GelMAC hydrogels, their corresponding *in vivo* hemostatic efficacy utilizing a rat liver bleeding model were studied and analyzed. Six experimental groups were tested which included four groups of bioadhesives (GelMA, GelMAC, GelMA-Fe, and GelMAC-Fe), and 2 control groups (injury only as negative control and commercially available SURGICEL® as the positive control). Immediately after creating a

standardized liver wound using a 2mm-biopsy punch, hemostatic bioadhesives were applied to the bleeding lesion and crosslinked for 4 min using visible light (Figure 4.5A-E). It should be noted that any blood loss from the incision site (from the time of incision to complete coagulation) was collected on a filter paper and weighted immediately after. It was observed that the GelMAC-Fe hydrogel was rapidly crosslinked and was able to stop the bleeding at a relatively shorter time compared to other experimental groups (Figure 4.5C). As shown in Figure 4.5F, SURGICEL® (positive control), GelMA, and GelMAC-Fe treated groups showed a significant reduction in bleeding in comparison to the untreated injury group. More specifically, GelMA and GelMAC-Fe groups demonstrated 36.2 ± 8.3, and 48.1 ± 4.9 % reduction in bleeding, respectively. Representative images of the collected blood mass on the filter paper are shown for each experimental group in Figure 4.5G. These representative images allow to further qualitatively analyze the mass of the blood collected which is in agreement with our quantitative measurements and analysis.

After stopping the bleeding, the animals treated by the commercial hemostatic agent (SURGICEL®) and the experimental groups were kept for one week to study the effect of material on the liver tissues. Injury group showed that scar tissue was formed at the injured site after one week. In the group treated by SURGICEL®, despite being able to effectively stop the bleeding during surgery, the hemostatic site was found discolored to yellowish color one week post-surgery indicating a mild immune response. All the experimental groups were effectively covered and remained adherence to the incision sites, with no abdominal organ adhesion or prominent discoloration observed. The small concentration of Fe^{3+} used in the formation of GelMA- and GelMAC-Fe hydrogels, did not demonstrate any toxicity *in vivo.* Overall, our results confirmed

the excellent hemostatic activity of GelMAC-Fe hydrogels through synergistic effect of catechol groups and ferric ions.

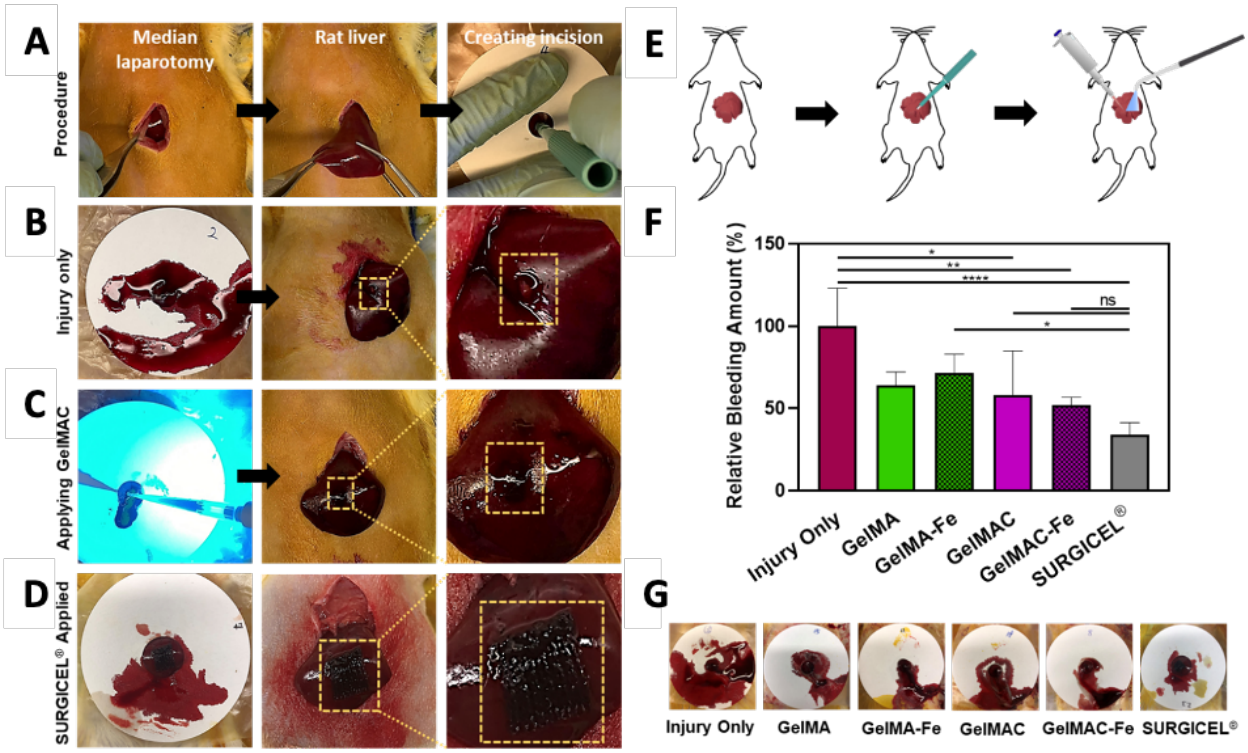

Figure 4.5 In vivo hemostatic efficacy of the sealants in a rat liver bleeding model. A) Images of the surgical procedure. **B)** Liver wound site post-puncture and without the utility of any treatment. **C)** Application, photocrosslinking, and the hemostatic ability of the GelMAC hydrogels at the wound site. **D)** Application of the commercial hemostatic agent SURGICEL®. **E)** A schematic depicting the application and photocrosslinking of the GelMA and GelMAC hydrogels. **F)** Relative bleeding amount for each study group in comparison to the blood mass collected on the filter paper for the injury only group. **G)** Representative images of the blood collected on the filter papers for each experimental group. Data are represented as mean ± SD (*$p < 0.05$, **$p < 0.01$, and ****$p < 0.0001$, n =4).

5. Conclusions

Sealants, hemostats, and adhesives have emerged as effective biomedical tools for surgical wound management, especially in minimally invasive surgeries. With the growing awareness about risks

of conventional surgeries, the need for new techniques for wound closure are increasing. Current approaches for wound management include using commercially available fibrin- cyanoacrylate- and/or collagen- reduced cellulose-based adhesives, which are associated with serious toxicity concerns as well as limited adhesive efficiency when used on wet surfaces. Therefore, new hydrogel-based wound management approaches suggested the use of polysaccharide-based adhesives (e.g., chitosan, dextran, alginate, and etc.) with hemostatic properties. However, their medical applications were limited according to pro-activation of the host tissue response after implantation. Gelatin (denatured collagen) is a cheap and highly biocompatible polymer that is derived from different sources (e.g., porcine, fish, bovine). Also, gelatin supports modification and crosslinking through different techniques according to the presence of various functional groups, which enabled us to control the physical and biological properties of the resulting gelatin-based hydrogel. After modification of gelatin in two consecutive reactions with dopamine and methacrylic anhydride, the swellability, degradation rate, mechanical, and adhesive properties of the hydrogels were tuned to form a double-crosslinked and photo-crosslinkable network (GelMAC-Fe hydrogel). In addition to the excellent cytocompatibility observed for the GelMAC-Fe hydrogel *in vitro*, it could also reduce the risk of fibrosis around hydrogel and improve the healing *in vivo*. Moreover, hemostatic efficiency of the GelMAC-Fe hydrogel was quantified and compared with commercially available hemostatic adhesive (SURGICEL®) using an *in vitro* coagulation test as well as an *in vivo* liver bleeding model. Our results confirmed the excellent hemostatic activity of GelMAC-Fe hydrogels through synergistic effect of catechol groups and ferric ions. Altogether, our proposed hydrogel system in this study can be used as a sutureless hemostatic sealant with great adhesion ability to different biological surfaces (i.e., liver, kidney, skin, intestine) in the presence of blood. Moreover, it is able to improve the cellular migration and

consequently healing as well. The future work will focus on evaluating the ability of this system to reduce the risk of infection after traumatic injury as well as incorporating a more physiologically relevant animal model for surgical wounds. This is mainly because wounds are highly susceptible to microbial infection and biofilm formation, especially in patients with impaired and dysfunctional immune system.

APPENDIX

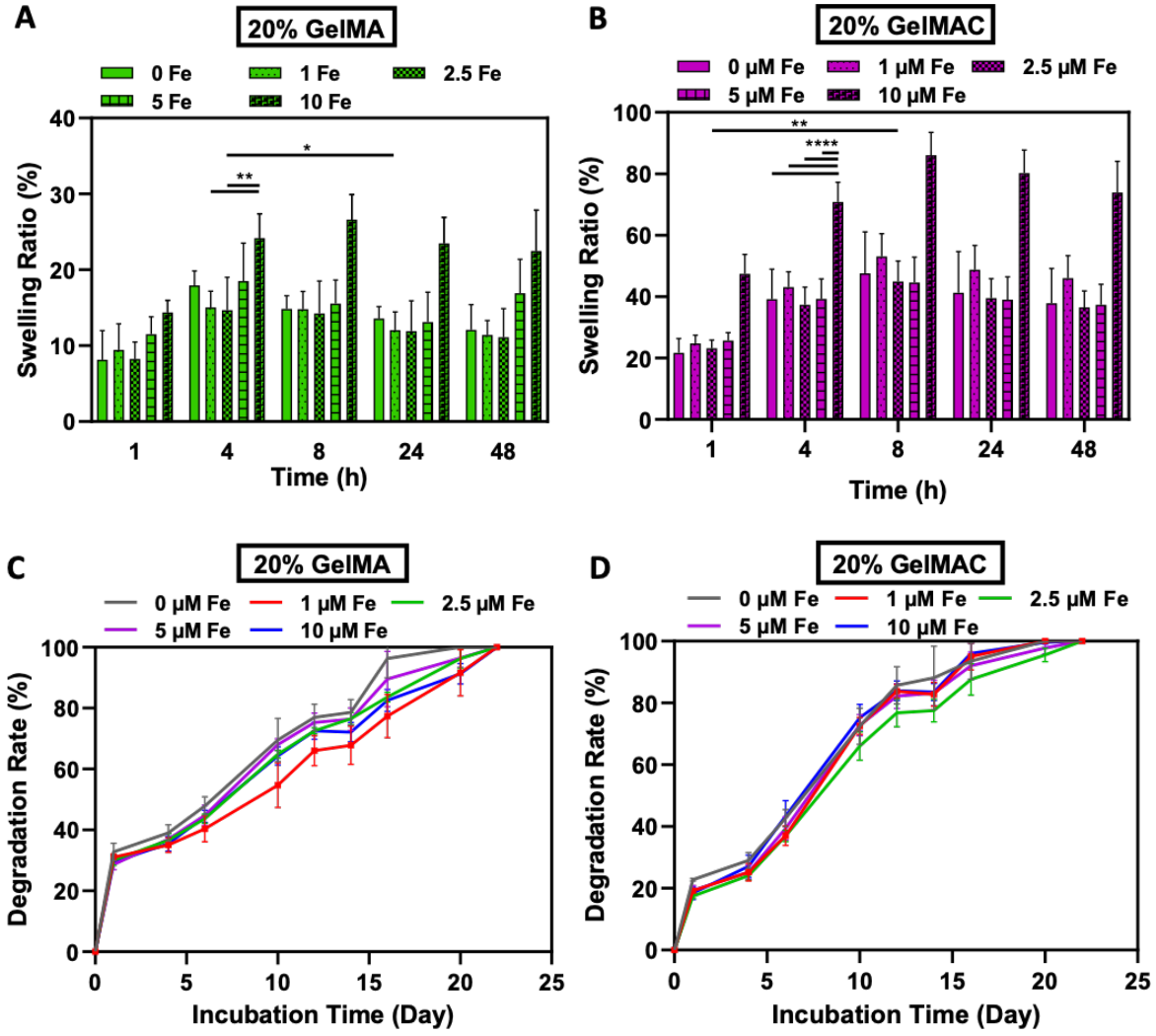

Figure A-1 Swelling and degradation profiles of GelMAC and GelMA hydrogels. A) Swelling ratio of GelMA hydrogels and **B)** Swelling ratio of GelMAC hydrogels containing various concentrations of ferric ions (Fe^{3+}) in DPBS. **C)** Degradation rate of GelMA hydrogels and **D)** Degradation rate of GelMAC hydrogels containing various concentrations of ferric ions (Fe^{3+}) in enzyme-containing DPBS solutions. Data are represented as mean ± SD (*<0.05, **$p < 0.01$, ***$p < 0.001$ and ****$p < 0.0001$, $n \geq 4$).

REFERENCES

[1] C.f.D. Control, Prevention, Surgical Site Infection (SSI) Event; 2017, Atlanta, GA: Centers for Disease Control and Prevention (2017).

[2] I. Galanakis, N. Vasdev, N. Soomro, A review of current hemostatic agents and tissue sealants used in laparoscopic partial nephrectomy, Reviews in urology 13(3) (2011) 131.

[3] W.D. Spotnitz, S. Burks, Hemostats, sealants, and adhesives: components of the surgical toolbox, Transfusion 48(7) (2008) 1502-1516.

[4] O. Chiara, S. Cimbanassi, G. Bellanova, M. Chiarugi, A. Mingoli, G. Olivero, S. Ribaldi, G. Tugnoli, S. Basilicò, F. Bindi, A systematic review on the use of topical hemostats in trauma and emergency surgery, BMC surgery 18(1) (2018) 68.

[5] N. Annabi, D. Rana, E. Shirzaei Sani, R. Portillo-Lara, J.L. Gifford, M.M. Fares, S.M. Mithieux, A.S. Weiss, Engineering a sprayable and elastic hydrogel adhesive with antimicrobial properties for wound healing, Biomaterials 139 (2017) 229-243.

[6] N. Lang, M.J. Pereira, Y. Lee, I. Friehs, N.V. Vasilyev, E.N. Feins, K. Ablasser, E.D. O'Cearbhaill, C. Xu, A. Fabozzo, A blood-resistant surgical glue for minimally invasive repair of vessels and heart defects, Science translational medicine 6(218) (2014) 218ra6-218ra6.

[7] M. Tavafoghi, A. Sheikhi, R. Tutar, J. Jahangiry, A. Baidya, R. Haghniaz, A. Khademhosseini, Engineering Tough, Injectable, Naturally Derived, Bioadhesive Composite Hydrogels, Advanced Healthcare Materials 9(10) (2020) 1901722.

[8] P. Kord Forooshani, B.P. Lee, Recent approaches in designing bioadhesive materials inspired by mussel adhesive protein, Journal of Polymer Science Part A: Polymer Chemistry 55(1) (2017) 9-33.

[9] H. Lee, N.F. Scherer, P.B. Messersmith, Single-molecule mechanics of mussel adhesion, Proceedings of the National Academy of Sciences 103(35) (2006) 12999-13003.

[10] M. Yu, J. Hwang, T.J. Deming, Role of L-3, 4-dihydroxyphenylalanine in mussel adhesive proteins, Journal of the American Chemical Society 121(24) (1999) 5825-5826.

[11] L. Han, Y. Zhang, X. Lu, K. Wang, Z. Wang, H. Zhang, Polydopamine nanoparticles modulating stimuli-responsive PNIPAM hydrogels with cell/tissue adhesiveness, ACS applied materials & interfaces 8(42) (2016) 29088-29100.

[12] H. Lee, J. Rho, P.B. Messersmith, Facile conjugation of biomolecules onto surfaces via mussel adhesive protein inspired coatings, Advanced Materials 21(4) (2009) 431-434.

[13] H. Zhang, L.P. Bré, T. Zhao, Y. Zheng, B. Newland, W. Wang, Mussel-inspired hyperbranched poly (amino ester) polymer as strong wet tissue adhesive, Biomaterials 35(2) (2014) 711-719.

[14] J. Yang, R. Bai, B. Chen, Z. Suo, Hydrogel Adhesion: A Supramolecular Synergy of Chemistry, Topology, and Mechanics, Advanced Functional Materials 30(2) (2020) 1901693.

[15] W. Zhang, R. Wang, Z. Sun, X. Zhu, Q. Zhao, T. Zhang, A. Cholewinski, F. Yang, B. Zhao, R. Pinnaratip, P.K. Forooshani, B.P. Lee, Catechol-functionalized hydrogels: biomimetic design, adhesion mechanism, and biomedical applications, Chemical Society Reviews 49(2) (2020) 433-464.

[16] W.-Y. Quan, Z. Hu, H.-Z. Liu, Q.-Q. Ouyang, D.-Y. Zhang, S.-D. Li, P.-W. Li, Z.-M. Yang, Mussel-Inspired Catechol-Functionalized Hydrogels and Their Medical Applications, Molecules 24(14) (2019) 2586.

[17] J.Y. Kim, S.B. Ryu, K.D. Park, Preparation and characterization of dual-crosslinked gelatin hydrogel via Dopa-Fe3+ complexation and fenton reaction, Journal of Industrial and Engineering Chemistry 58 (2018) 105-112.

[18] A.M. Behrens, M.J. Sikorski, P. Kofinas, Hemostatic strategies for traumatic and surgical bleeding, Journal of Biomedical Materials Research Part A 102(11) (2014) 4182-4194.

[19] Y. Hong, F. Zhou, Y. Hua, X. Zhang, C. Ni, D. Pan, Y. Zhang, D. Jiang, L. Yang, Q. Lin, A strongly adhesive hemostatic hydrogel for the repair of arterial and heart bleeds, Nature communications 10(1) (2019) 1-11.

[20] T.A. Ostomel, Q. Shi, P.K. Stoimenov, G.D. Stucky, Metal oxide surface charge mediated hemostasis, Langmuir 23(22) (2007) 11233-11238.

[21] B. Bordes, D. Martin, B. Schloss, A. Beebe, W. Samora, J. Klamar, D. Stukus, J.D. Tobias, Intraoperative anaphylactic reaction: is it the Floseal?, The Journal of Pediatric Pharmacology and Therapeutics 21(4) (2016) 358-365.

[22] L. Wang, X. Zhang, K. Yang, Y.V. Fu, T. Xu, S. Li, D. Zhang, L.N. Wang, C.S. Lee, A Novel Double-Crosslinking-Double-Network Design for Injectable Hydrogels with Enhanced Tissue Adhesion and Antibacterial Capability for Wound Treatment, Advanced Functional Materials 30(1) (2020) 1904156.

[23] J. Jennings, Controlling chitosan degradation properties in vitro and in vivo, Chitosan Based Biomaterials Volume 1, Elsevier2017, pp. 159-182.

[24] C.A. Tyson, A.E. Martell, Equilibriums of metal ions with pyrocatechol and 3, 5-di-tert-butylpyrocatechol, Journal of the American Chemical Society 90(13) (1968) 3379-3386.

[25] B.A. Borgias, S.R. Cooper, Y.B. Koh, K.N. Raymond, Synthetic, structural, and physical studies of titanium complexes of catechol and 3, 5-di-tert-butylcatechol, Inorganic Chemistry 23(8) (1984) 1009-1016.

[26] E. Caló, V.V. Khutoryanskiy, Biomedical applications of hydrogels: A review of patents and commercial products, European Polymer Journal 65 (2015) 252-267.

[27] Q. Chai, Y. Jiao, X. Yu, Hydrogels for Biomedical Applications: Their Characteristics and the Mechanisms behind Them, Gels 3(1) (2017) 6.

[28] T.R. Hoare, D.S. Kohane, Hydrogels in drug delivery: Progress and challenges, Polymer 49(8) (2008) 1993-2007.

[29] G.-L. Ying, N. Jiang, S. Maharjan, Y.-X. Yin, R.-R. Chai, X. Cao, J.-Z. Yang, A.K. Miri, S. Hassan, Y.S. Zhang, Aqueous Two-Phase Emulsion Bioink-Enabled 3D Bioprinting of Porous Hydrogels, Advanced Materials 30(50) (2018) 1805460.

[30] F. Antonio, P. Petya, T. Tzanko, Hydrogel Dressings for Advanced Wound Management, Current Medicinal Chemistry 25(41) (2018) 5782-5797.

[31] A.Y. Clark, K.E. Martin, J.R. García, C.T. Johnson, H.S. Theriault, W.M. Han, D.W. Zhou, E.A. Botchwey, A.J. García, Integrin-specific hydrogels modulate transplanted human bone marrow-derived mesenchymal stem cell survival, engraftment, and reparative activities, Nature Communications 11(1) (2020) 114.

[32] S. Das, B. Basu, An Overview of Hydrogel-Based Bioinks for 3D Bioprinting of Soft Tissues, Journal of the Indian Institute of Science 99(3) (2019) 405-428.

[33] L.R. Nih, P. Moshayedi, I.L. Llorente, A.R. Berg, J. Cinkornpumin, W.E. Lowry, T. Segura, S.T. Carmichael, Engineered HA hydrogel for stem cell transplantation in the brain: Biocompatibility data using a design of experiment approach, Data in Brief 10 (2017) 202-209.

[34] J.M. Oliveira, L. Carvalho, J. Silva-Correia, S. Vieira, M. Majchrzak, B. Lukomska, L. Stanaszek, P. Strymecka, I. Malysz-Cymborska, D. Golubczyk, L. Kalkowski, R.L. Reis, M. Janowski, P. Walczak, Hydrogel-based scaffolds to support intrathecal stem cell transplantation as a gateway to the spinal cord: clinical needs, biomaterials, and imaging technologies, npj Regenerative Medicine 3(1) (2018) 8.

[35] J.M. Unagolla, A.C. Jayasuriya, Hydrogel-based 3D bioprinting: A comprehensive review on cell-laden hydrogels, bioink formulations, and future perspectives, Applied Materials Today 18 (2020) 100479.

[36] Q. Xu, M. Chang, Y. Zhang, E. Wang, M. Xing, L. Gao, Z. Huan, F. Guo, J. Chang, PDA/Cu Bioactive Hydrogel with "Hot Ions Effect" for Inhibition of Drug-Resistant Bacteria and Enhancement of Infectious Skin Wound Healing, ACS Applied Materials & Interfaces 12(28) (2020) 31255-31269.

[37] X. Xu, L. Che, L. Xu, D. Huang, J. Wu, Z. Du, Y. Lin, X. Hu, Q. Zhao, Z. Lin, L. Xu, Green preparation of anti-inflammation an injectable 3D porous hydrogel for speeding up deep second-degree scald wound healing, RSC Advances 10(59) (2020) 36101-36110.

[38] N. Pandey, L.F. Soto-Garcia, J. Liao, Z. Philippe, K.T. Nguyen, Y. Hong, Mussel-inspired bioadhesives in healthcare: design parameters, current trends, and future perspectives, Biomaterials Science 8(5) (2020) 1240-1255.

[39] R. Pinnaratip, M.S.A. Bhuiyan, K. Meyers, R.M. Rajachar, B.P. Lee, Multifunctional Biomedical Adhesives, Advanced Healthcare Materials 8(11) (2019) 1801568.

[40] G.M. Taboada, K. Yang, M.J.N. Pereira, S.S. Liu, Y. Hu, J.M. Karp, N. Artzi, Y. Lee, Overcoming the translational barriers of tissue adhesives, Nature Reviews Materials 5(4) (2020) 310-329.

[41] C. Vasile, D. Pamfil, E. Stoleru, M. Baican, New Developments in Medical Applications of Hybrid Hydrogels Containing Natural Polymers, Molecules 25(7) (2020) 1539.

[42] B. Yang, S. Jin, Y. Park, Y.M. Jung, H.J. Cha, Coacervation of Interfacial Adhesive Proteins for Initial Mussel Adhesion to a Wet Surface, Small 14(52) (2018) 1803377.

[43] E. Shirzaei Sani, R. Portillo-Lara, A. Spencer, W. Yu, B.M. Geilich, I. Noshadi, T.J. Webster, N. Annabi, Engineering Adhesive and Antimicrobial Hyaluronic Acid/Elastin-like Polypeptide Hybrid Hydrogels for Tissue Engineering Applications, ACS Biomaterials Science & Engineering 4(7) (2018) 2528-2540.

[44] N. Annabi, Y.-N. Zhang, A. Assmann, E.S. Sani, G. Cheng, A.D. Lassaletta, A. Vegh, B. Dehghani, G.U. Ruiz-Esparza, X. Wang, S. Gangadharan, A.S. Weiss, A. Khademhosseini, Engineering a highly elastic human protein–based sealant for surgical applications, Science Translational Medicine 9(410) (2017) eaai7466.

[45] N. Annabi, S.M. Mithieux, P. Zorlutuna, G. Camci-Unal, A.S. Weiss, A. Khademhosseini, Engineered cell-laden human protein-based elastomer, Biomaterials 34(22) (2013) 5496-505.

[46] M.M. Hasani-Sadrabadi, P. Sarrion, S. Pouraghaei, Y. Chau, S. Ansari, S. Li, T. Aghaloo, A. Moshaverinia, An engineered cell-laden adhesive hydrogel promotes craniofacial bone tissue regeneration in rats, Science Translational Medicine 12(534) (2020) eaay6853.

[47] Y. Liu, B.P. Lee, Recovery property of double-network hydrogel containing a mussel-inspired adhesive moiety and nano-silicate, Journal of Materials Chemistry B 4(40) (2016) 6534-6540.

[48] Y. Liu, H. Meng, S. Konst, R. Sarmiento, R. Rajachar, B.P. Lee, Injectable Dopamine-Modified Poly(ethylene glycol) Nanocomposite Hydrogel with Enhanced Adhesive Property and Bioactivity, ACS Applied Materials & Interfaces 6(19) (2014) 16982-16992.

[49] Y. Liu, H. Meng, Z. Qian, N. Fan, W. Choi, F. Zhao, B.P. Lee, A Moldable Nanocomposite Hydrogel Composed of a Mussel-Inspired Polymer and a Nanosilicate as a Fit-to-Shape Tissue Sealant, Angewandte Chemie International Edition 56(15) (2017) 4224-4228.

[50] N. Annabi, S.R. Shin, A. Tamayol, M. Miscuglio, M.A. Bakooshli, A. Assmann, P. Mostafalu, J.-Y. Sun, S. Mithieux, L. Cheung, X. Tang, A.S. Weiss, A. Khademhosseini, Highly Elastic and Conductive Human-Based Protein Hybrid Hydrogels, Advanced Materials 28(1) (2016) 40-49.

[51] I. Noshadi, B.W. Walker, R. Portillo-Lara, E. Shirzaei Sani, N. Gomes, M.R. Aziziyan, N. Annabi, Engineering Biodegradable and Biocompatible Bio-ionic Liquid Conjugated Hydrogels with Tunable Conductivity and Mechanical Properties, Scientific Reports 7(1) (2017) 4345.

[52] N. Lang, M.J. Pereira, Y. Lee, I. Friehs, N.V. Vasilyev, E.N. Feins, K. Ablasser, E.D. O'Cearbhaill, C. Xu, A. Fabozzo, R. Padera, S. Wasserman, F. Freudenthal, L.S. Ferreira, R. Langer, J.M. Karp, P.J. del Nido, A Blood-Resistant Surgical Glue for Minimally Invasive Repair of Vessels and Heart Defects, Science Translational Medicine 6(218) (2014) 218ra6-218ra6.

[53] J. Li, A.D. Celiz, J. Yang, Q. Yang, I. Wamala, W. Whyte, B.R. Seo, N.V. Vasilyev, J.J. Vlassak, Z. Suo, D.J. Mooney, Tough adhesives for diverse wet surfaces, Science 357(6349) (2017) 378-381.

[54] K.L. Fujimoto, K. Tobita, J. Guan, R. Hashizume, K. Takanari, C.M. Alfieri, K.E. Yutzey, W.R. Wagner, Placement of an elastic biodegradable cardiac patch on a subacute infarcted heart leads to cellularization with early developmental cardiomyocyte characteristics, J Card Fail 18(7) (2012) 585-95.

[55] S.A. Guelcher, K.M. Gallagher, J.E. Didier, D.B. Klinedinst, J.S. Doctor, A.S. Goldstein, G.L. Wilkes, E.J. Beckman, J.O. Hollinger, Synthesis of biocompatible segmented polyurethanes from aliphatic diisocyanates and diurea diol chain extenders, Acta Biomaterialia 1(4) (2005) 471-484.

[56] L. Montanaro, C.R. Arciola, E. Cenni, G. Ciapetti, F. Savioli, F. Filippini, L.A. Barsanti, Cytotoxicity, blood compatibility and antimicrobial activity of two cyanoacrylate glues for surgical use, Biomaterials 22(1) (2000) 59-66.

[57] A.J. Singer, H.C. Thode, A review of the literature on octylcyanoacrylate tissue adhesive, The American Journal of Surgery 187(2) (2004) 238-248.

[58] D.H. Sierra, A.W. Eberhardt, J.E. Lemons, Failure characteristics of multiple-component fibrin-based adhesives, Journal of Biomedical Materials Research 59(1) (2002) 1-11.

[59] X. Xie, J.-k. Tian, F.-q. Lv, R. Wu, W.-b. Tang, Y.-k. Luo, Y.-q. Huang, J. Tang, A novel hemostatic sealant composed of gelatin, transglutaminase and thrombin effectively controls liver trauma-induced bleeding in dogs, Acta Pharmacologica Sinica 34(7) (2013) 983-988.

[60] S. An, E.J. Jeon, J. Jeon, S.-W. Cho, A serotonin-modified hyaluronic acid hydrogel for multifunctional hemostatic adhesives inspired by a platelet coagulation mediator, Materials Horizons 6(6) (2019) 1169-1178.

[61] H. Zhu, X. Mei, Y. He, H. Mao, W. Tang, R. Liu, J. Yang, K. Luo, Z. Gu, L. Zhou, Fast and High Strength Soft Tissue Bioadhesives Based on a Peptide Dendrimer with Antimicrobial Properties and Hemostatic Ability, ACS Applied Materials & Interfaces 12(4) (2020) 4241-4253.

[62] Y. Shou, J. Zhang, S. Yan, P. Xia, P. Xu, G. Li, K. Zhang, J. Yin, Thermoresponsive Chitosan/DOPA-Based Hydrogel as an Injectable Therapy Approach for Tissue-Adhesion and Hemostasis, ACS Biomaterials Science & Engineering 6(6) (2020) 3619-3629.

[63] Y. Liang, X. Zhao, T. Hu, B. Chen, Z. Yin, P.X. Ma, B. Guo, Adhesive Hemostatic Conducting Injectable Composite Hydrogels with Sustained Drug Release and Photothermal Antibacterial Activity to Promote Full-Thickness Skin Regeneration During Wound Healing, Small 15(12) (2019) 1900046.

[64] C. Cui, C. Fan, Y. Wu, M. Xiao, T. Wu, D. Zhang, X. Chen, B. Liu, Z. Xu, B. Qu, W. Liu, Water-Triggered Hyperbranched Polymer Universal Adhesives: From Strong Underwater Adhesion to Rapid Sealing Hemostasis, Advanced Materials 31(49) (2019) 1905761.

[65] Y. Hong, F. Zhou, Y. Hua, X. Zhang, C. Ni, D. Pan, Y. Zhang, D. Jiang, L. Yang, Q. Lin, Y. Zou, D. Yu, D.E. Arnot, X. Zou, L. Zhu, S. Zhang, H. Ouyang, A strongly adhesive hemostatic hydrogel for the repair of arterial and heart bleeds, Nature Communications 10(1) (2019) 2060.

[66] S. Bai, X. Zhang, P. Cai, X. Huang, Y. Huang, R. Liu, M. Zhang, J. Song, X. Chen, H. Yang, A silk-based sealant with tough adhesion for instant hemostasis of bleeding tissues, Nanoscale Horizons (2019).

[67] J.-S. Jhiang, T.-H. Wu, C.-J. Chou, Y. Chang, C.-J. Huang, Gel-like ionic complexes for antimicrobial, hemostatic and adhesive properties, Journal of Materials Chemistry B 7(17) (2019) 2878-2887.

[68] D. Zhang, Z. Xu, H. Li, C. Fan, C. Cui, T. Wu, M. Xiao, Y. Yang, J. Yang, W. Liu, Fabrication of strong hydrogen-bonding induced coacervate adhesive hydrogels with antibacterial and hemostatic activities, Biomaterials Science 8(5) (2020) 1455-1463.

[69] J. He, M. Shi, Y. Liang, B. Guo, Conductive adhesive self-healing nanocomposite hydrogel wound dressing for photothermal therapy of infected full-thickness skin wounds, Chemical Engineering Journal (2020) 124888.

[70] L. Gao, S. Ma, J. Luo, G. Bao, Y. Wu, F. Zhou, Y. Liang, Synthesizing Functional Biomacromolecular Wet Adhesives with Typical Gel–Sol Transition and Shear-Thinning Features, ACS Biomaterials Science & Engineering 5(9) (2019) 4293-4301.

[71] M. Suneetha, K.M. Rao, S.S. Han, Mussel-Inspired Cell/Tissue-Adhesive, Hemostatic Hydrogels for Tissue Engineering Applications, ACS Omega 4(7) (2019) 12647-12656.

[72] Y.-F. Shen, J.-H. Huang, Z.-E. Wu, K.-Y. Wang, J. Zheng, L. Cai, X.-L. Li, H. Gao, X.-Y. Jin, J.-F. Li, Cationic superabsorbent hydrogel composed of mesoporous silica as a potential haemostatic material, Materials Science and Engineering: C (2020) 110841.

[73] V. Krishnadoss, A. Melillo, B. Kanjilal, T. Hannah, E. Ellis, A. Kapetanakis, J. Hazelton, J. San Roman, A. Masoumi, J. Leijten, Bioionic Liquid Conjugation as Universal Approach To Engineer Hemostatic Bioadhesives, ACS applied materials & interfaces 11(42) (2019) 38373-38384.

[74] J.L. Daristotle, S.T. Zaki, L.W. Lau, L. Torres Jr, A. Zografos, P. Srinivasan, O.B. Ayyub, A.D. Sandler, P. Kofinas, Improving the adhesion, flexibility, and hemostatic efficacy of a sprayable polymer blend surgical sealant by incorporating silica particles, Acta biomaterialia 90 (2019) 205-216.

[75] Y. Liang, X. Zhao, T. Hu, Y. Han, B. Guo, Mussel-inspired, antibacterial, conductive, antioxidant, injectable composite hydrogel wound dressing to promote the regeneration of infected skin, Journal of colloid and interface science 556 (2019) 514-528.

[76] R. Campos-Cuerva, B. Fernández-Muñoz, F. Farfán López, S. Pereira Arenas, M. Santos-González, L. Lopez-Navas, M. Alaminos, A. Campos, J. Muntané, C. Cepeda-Franco, Nanostructured fibrin agarose hydrogel as a novel haemostatic agent, Journal of tissue engineering and regenerative medicine 13(4) (2019) 664-673.

[77] C.K. Song, M.-K. Kim, J. Lee, E. Davaa, R. Baskaran, S.-G. Yang, Dopa-Empowered Schiff Base Forming Alginate Hydrogel Glue for Rapid Hemostatic Control, Macromolecular Research 27(2) (2019) 119-125.

[78] E. Park, J. Lee, K.M. Huh, S.H. Lee, H. Lee, Toxicity-Attenuated Glycol Chitosan Adhesive Inspired by Mussel Adhesion Mechanisms, Advanced healthcare materials 8(14) (2019) 1900275.

[79] H. Yuan, L. Chen, F.F. Hong, A biodegradable antibacterial nanocomposite based on oxidized bacterial nanocellulose for rapid hemostasis and wound healing, ACS Applied Materials & Interfaces 12(3) (2019) 3382-3392.

[80] Y. Liang, X. Zhao, T. Hu, B. Chen, Z. Yin, P.X. Ma, B. Guo, Adhesive Hemostatic Conducting Injectable Composite Hydrogels with Sustained Drug Release and Photothermal Antibacterial Activity to Promote Full-Thickness Skin Regeneration During Wound Healing, Small 15(12) (2019) 1900046.

[81] H. Zhu, X. Mei, Y. He, H. Mao, W. Tang, R. Liu, J. Yang, K. Luo, Z. Gu, L. Zhou, Fast and High Strength Soft Tissue Bioadhesives Based on a Peptide Dendrimer with Antimicrobial Properties and Hemostatic Ability, ACS Applied Materials & Interfaces 12(4) (2019) 4241-4253.

[82] Y. Shou, J. Zhang, S. Yan, P. Xia, P. Xu, G. Li, K. Zhang, J. Yin, Thermoresponsive Chitosan/DOPA-Based Hydrogel as an Injectable Therapy Approach for Tissue-Adhesion and Hemostasis, ACS Biomaterials Science & Engineering (2020).

[83] A. Nishiguchi, Y. Kurihara, T. Taguchi, Hemostatic, Tissue-Adhesive Colloidal Wound Dressing Functionalized by UV Irradiation, ACS Applied Bio Materials 3(3) (2020) 1705-1711.

[84] X. Du, Y. Liu, H. Yan, M. Rafique, S. Li, X. Shan, L. Wu, M. Qiao, D. Kong, L. Wang, Anti-Infective and Pro-Coagulant Chitosan-Based Hydrogel Tissue Adhesive for Sutureless Wound Closure, Biomacromolecules 21(3) (2020) 1243-1253.

[85] C. Cui, C. Fan, Y. Wu, M. Xiao, T. Wu, D. Zhang, X. Chen, B. Liu, Z. Xu, B. Qu, Water-Triggered Hyperbranched Polymer Universal Adhesives: From Strong Underwater Adhesion to Rapid Sealing Hemostasis, Advanced materials 31(49) (2019) 1905761.

[86] Y. Hong, F. Zhou, Y. Hua, X. Zhang, C. Ni, D. Pan, Y. Zhang, D. Jiang, L. Yang, Q. Lin, A strongly adhesive hemostatic hydrogel for the repair of arterial and heart bleeds, Nature communications 10(1) (2019) 2060.

[87] C. Liu, X. Liu, C. Liu, N. Wang, H. Chen, W. Yao, G. Sun, Q. Song, W. Qiao, A highly efficient, in situ wet-adhesive dextran derivative sponge for rapid hemostasis, Biomaterials 205 (2019) 23-37.

[88] K. Yue, X. Li, K. Schrobback, A. Sheikhi, N. Annabi, J. Leijten, W. Zhang, Y.S. Zhang, D.W. Hutmacher, T.J. Klein, A. Khademhosseini, Structural analysis of photocrosslinkable methacryloyl-modified protein derivatives, Biomaterials 139 (2017) 163-171.

[89] X. Zhou, Z. Luo, A. Baidya, H.-j. Kim, C. Wang, X. Jiang, M. Qu, J. Zhu, L. Ren, F. Vajhadin, P. Tebon, N. Zhang, Y. Xue, Y. Feng, C. Xue, Y. Chen, K. Lee, J. Lee, S. Zhang, C. Xu, N. Ashammakhi, S. Ahadian, M.R. Dokmeci, Z. Gu, W. Sun, A. Khademhosseini, Biodegradable β-Cyclodextrin Conjugated Gelatin Methacryloyl Microneedle for Delivery of Water-Insoluble Drug, Advanced Healthcare Materials 9(11) (2020) 2000527.

[90] K. Yue, X. Li, K. Schrobback, A. Sheikhi, N. Annabi, J. Leijten, W. Zhang, Y.S. Zhang, D.W. Hutmacher, T.J. Klein, Structural analysis of photocrosslinkable methacryloyl-modified protein derivatives, Biomaterials 139 (2017) 163-171.

[91] A. Assmann, A. Vegh, M. Ghasemi-Rad, S. Bagherifard, G. Cheng, E.S. Sani, G.U. Ruiz-Esparza, I. Noshadi, A.D. Lassaletta, S. Gangadharan, A highly adhesive and naturally derived sealant, Biomaterials 140 (2017) 115-127.

[92] J. Guo, W. Sun, J.P. Kim, X. Lu, Q. Li, M. Lin, O. Mrowczynski, E.B. Rizk, J. Cheng, G. Qian, Development of tannin-inspired antimicrobial bioadhesives, Acta biomaterialia 72 (2018) 35-44.

[93] T. Yadav, V. Mukherjee, Interpretation of IR and Raman spectra of dopamine neurotransmitter and effect of hydrogen bond in HCl, Journal of Molecular Structure 1160 (2018) 256-270.

[94] M.A. Gebbie, W. Wei, A.M. Schrader, T.R. Cristiani, H.A. Dobbs, M. Idso, B.F. Chmelka, J.H. Waite, J.N. Israelachvili, Tuning underwater adhesion with cation–π interactions, Nature Chemistry 9(5) (2017) 473-479.

[95] D.S. Hwang, H. Zeng, A. Masic, M.J. Harrington, J.N. Israelachvili, J.H. Waite, Protein-and metal-dependent interactions of a prominent protein in mussel adhesive plaques, Journal of biological chemistry (2010) jbc. M110. 133157.

[96] Q. Xing, K. Yates, C. Vogt, Z. Qian, M.C. Frost, F. Zhao, Increasing mechanical strength of gelatin hydrogels by divalent metal ion removal, Scientific reports 4 (2014) 4706.

[97] S. Hou, P.X. Ma, Stimuli-responsive supramolecular hydrogels with high extensibility and fast self-healing via precoordinated mussel-inspired chemistry, Chemistry of Materials 27(22) (2015) 7627-7635.

[98] A. Al-Mayah, J. Moseley, M. Velec, K.K. Brock, Sliding characteristic and material compressibility of human lung: Parametric study and verification, Medical Physics 36(10) (2009) 4625-4633.

[99] W. Carver, E.C. Goldsmith, Regulation of tissue fibrosis by the biomechanical environment, Biomed Res Int 2013 (2013) 101979-101979.

[100] Z. Xu, Mechanics of metal-catecholate complexes: the roles of coordination state and metal types, Scientific reports 3 (2013) 2914.

[101] M.S. Menyo, C.J. Hawker, J.H. Waite, Versatile tuning of supramolecular hydrogels through metal complexation of oxidation-resistant catechol-inspired ligands, Soft Matter 9(43) (2013) 10314-10323.

[102] E. Filippidi, T.R. Cristiani, C.D. Eisenbach, J.H. Waite, J.N. Israelachvili, B.K. Ahn, M.T. Valentine, Toughening elastomers using mussel-inspired iron-catechol complexes, Science 358(6362) (2017) 502-505.

[103] M. Shin, J.H. Ryu, K. Kim, M.J. Kim, S. Jo, M.S. Lee, D.Y. Lee, H. Lee, Hemostatic swabs containing polydopamine-like catecholamine chitosan-catechol for normal and coagulopathic animal models, ACS Biomaterials Science & Engineering 4(7) (2018) 2314-2318.

[104] M. Shin, S.-G. Park, B.-C. Oh, K. Kim, S. Jo, M.S. Lee, S.S. Oh, S.-H. Hong, E.-C. Shin, K.-S. Kim, Complete prevention of blood loss with self-sealing haemostatic needles, Nature materials 16(1) (2017) 147-152.

[105] Y. Zhao, B. Gao, H. Shon, B. Cao, J.-H. Kim, Coagulation characteristics of titanium (Ti) salt coagulant compared with aluminum (Al) and iron (Fe) salts, Journal of hazardous materials 185(2-3) (2011) 1536-1542.

[106] M.-B.A. Ashour, S.J. Gee, B.D. Hammock, Use of a 96-well microplate reader for measuring routine enzyme activities, Analytical Biochemistry 166(2) (1987) 353-360.